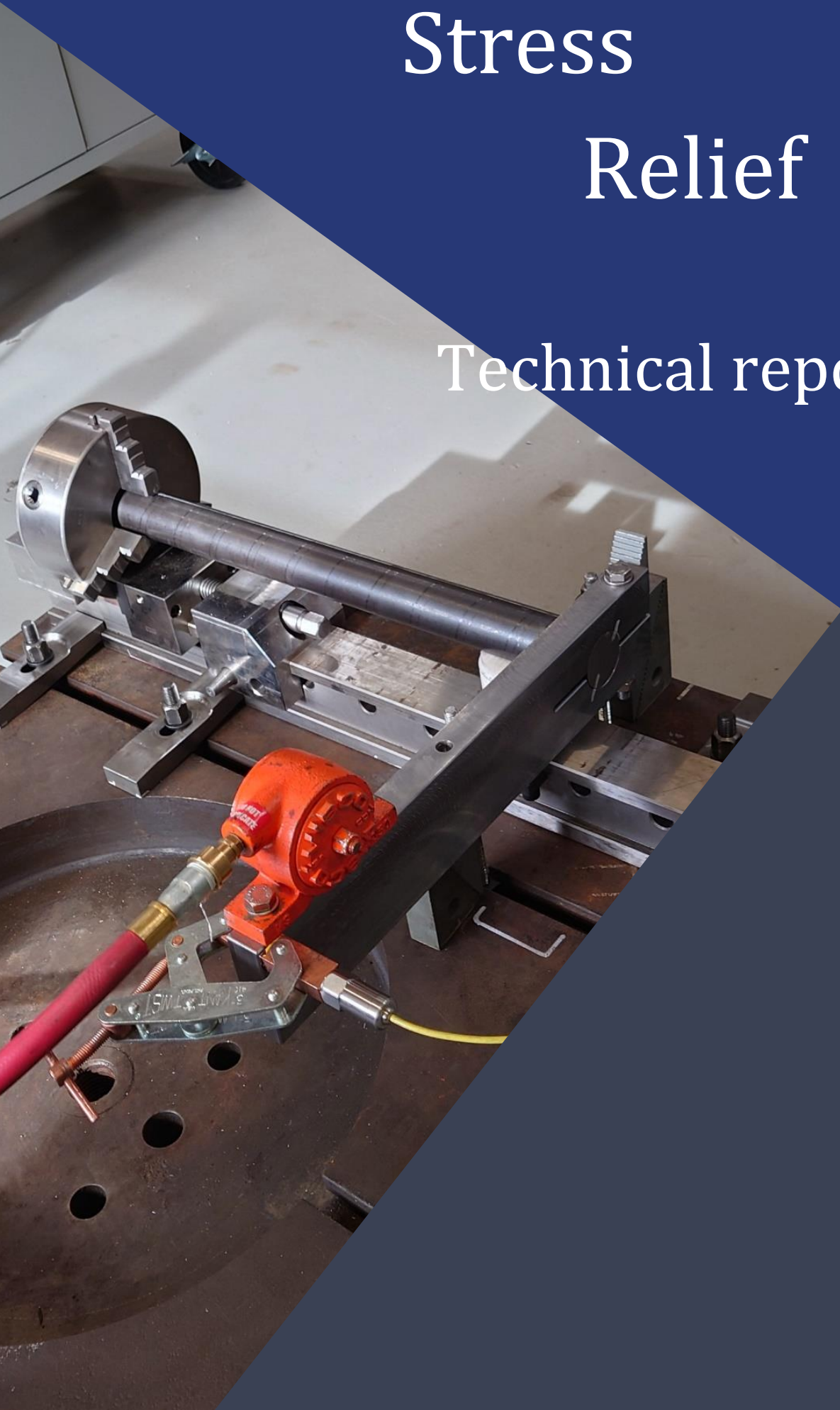


# Torsional Stress

# Relief

Technical report



## 1 Indhold

- This project is made in collaboration with: ..... 3
- Executive Summary..... 4
- 2 Introduction ..... 5
- 3 Pre-Analysis and Literature Study..... 5
- 4 Hypothesis..... 6
- 5 Success Criteria ..... 6
- 6 Project Scope ..... 6
- 7 Risk Analysis ..... 6
- 8 Experiment Design ..... 7
- 9 Experimental Procedure ..... 7
  - 9.1 Natural frequencies versus residual stress ..... 8
- 10 Design of test set-up ..... 8
  - 10.1 NATURAL FREQUENCY OF THE SYSTEM..... 9
  - 10.2 PNEUMATIC TURBINE MOTOR VS-250 – FORCE AND RPM ANALYSIS..... 12
  - 10.3 Flexural (VSR) treatment set-up..... 17
  - 10.4 Re-stressing of de-stressed bars ..... 18
  - 10.5 Taptesting..... 20
  - 10.6 Introduction..... 20
  - 10.7 Methodology..... 23
  - 10.8 Results ..... 24
  - 10.9 Conclusion on tap testing..... 33
- 11 Results of torsional and flexural tests..... 34
  - 11.1 Results of testing  $\varnothing$ 50 mm bars ..... 34
  - 11.2 Results of testing  $\varnothing$ 25 mm long bars ..... 36
  - 11.3 Results of testing  $\varnothing$ 25 mm short bars..... 37
  - 11.4 Test of 1. rod before and after treatment ..... 38
  - 11.5 Test of 2. Rod (control)..... 38
  - 11.6 Test of 3. Rod after treatment ..... 40
  - 11.7 Test of 4. Rod (control)..... 40
  - 11.8 Analysis of test results..... 41
- 12 Discussion..... 42
- 13 Conclusion..... 43

14	Dissemination .....	43
15	References .....	44
16	Appendix: Order confirmation Ø25 mm bars .....	45
	List of Figures .....	46
	List of Tables .....	47
17	Bibliografi .....	47

**This project is made in collaboration with:**

**Funding:**

- Industriens Fond
- Miljø- og Energifonden

**Contributors:**

- Tibnor

## Executive Summary

In 2015, DAMRC brought the Vibratory Stress Relief (VSR) technology to Denmark from the USA, where it has been used since 2000 to reduce residual stresses in metals using vibration.

Many machining companies use the conventional material normalization method of thermal annealing of workpieces (Thermal Stress Relief - TSR), which requires large amounts of energy in the annealing process, long treatment time and requires workpiece transportation to/from the annealing furnaces.

The aim of the P1001-04-08 Torsional Stress Relief (TorSR) project is to develop a new VSR-inspired system that uses torsional oscillations (twisting) to reduce residual stresses in rod materials instead of the flexural vibration superposition of structures. In literature, it has been found that there are cases where torsional stress relief is capable of showing a positive effect on some materials and geometries.

Three series of tests were made in order to show the capability of torsion treatment of residual stresses. These test series were designed to investigate effect of the aspect ratio and partly also to show the effectiveness of torsional versus flexural (VSR) residual stress treatment. The cold drawn bars should have stress already when delivered.

Though, since the bars have been on stock for some time before delivered to DAMRC it is not known to which degree they still had significant residual stresses when tested since DAMRC does not have access to stress measurement equipment. Getting access to the relevant stress measurements equipment is difficult since it is only available few places in the world. – as the most suitable equipment is expensive and does not guarantee full reliable results. To ensure that stresses were present at the testing, efforts were made to induce stresses in the bars. These efforts were of both thermal and mechanical type and are both well known to cause stresses in materials in many cases.

Though, it was not possible to demonstrate a reduction in residual stress neither through torsional nor flexural treatment of the bars when compared to no treatment at all. This, despite various efforts on ensuring the success of treatment already in the planning phase with e.g. characterisation of vibrator through tests and finite element (FEM) analysis of the necessary load to achieve large enough loads on the bars to obtain stress relaxation.

There are mainly three questions to be contemplated after the tests, were there at all significant residual stresses to reduce present in the bars, is the torsional and flexural vibration capable of reducing stresses in these bars and is the taptesting method a reliable way of indicating changes in residual stress? The answer on these questions were not demonstrated reliably through the testing. In some of the tests it seemed that there was a positive effect of the torsional vibration but too small for the taptesting to demonstrate clearly. Validating the taptest equipments capability of reducing residual stresses or making use of other methods for stress measurement is crucial for later tests of residual stress reduction. Further, more elaboration on results achieved externally on which materials that can be stress relieved can be a way to ensure that a clear result can be achieved.

## 2 Introduction

In 2015, DAMRC brought the Vibratory Stress Relief (VSR) technology to Denmark from the USA, where it has been used since 2000 to reduce residual stresses in metals using vibration.

Many machining companies use the conventional material normalization method of thermal annealing of workpieces (Thermal Stress Relief - TSR), which requires large amounts of energy in the annealing process, long treatment time and requires workpiece transportation to/from the annealing furnaces.

VSR technology does not add heat to the material - nor does it change the grain structure of the metal. The residual stresses of the material are reduced, as demonstrated in e.g. (Walker, 1995), by superimposing vibrations in the material, which by the dynamic action eliminate the dislocations in the metal's wear planes caused by the stress action occurring during fabrication. VSR technology also has the advantage of being a mobile processing device that can easily be transported to the workpiece. Thus, using VSR saves storage/laydown time, heavy transport, time in terms of easier machining and, compared to the thermal method, energy savings of between 72% - 95% are achieved for parts between 40 kg and 126 tons, according to our preliminary research activities.

Since 2015, we have been working on bringing the technology into industrial use, and this has been done on a variety of parts and have been especially successful on cast parts and large structures (e.g., wind turbine nacelles and towers). We have also had to acknowledge that the VSR technology in several cases has not had the desired effect on parts with high aspect ratio, i.e., parts where the largest main dimension is much larger than the smallest main dimension, e.g., rod materials. Rod materials play an essential role in structures for the automotive and energy sector, including shafts, cooling, and drives.

The aim of the P1001-04-08 Torsional Stress Relief (TorSR) project is to develop a new VSR-inspired system that uses torsional oscillations (twisting) to reduce residual stresses in rod materials instead of the flexural vibration superposition of structures. The project takes the form of a "pre-project", where a test setup will be developed that uses torsional oscillations as a technique to reduce residual stresses in rod materials. The aim is to validate the proposed stress relief method as viable for industrial applications, with the potential of testing the method and technology in case studies involving participating companies. Torsional stress relief has been investigated quite sparsely but some publications exist pointing at possibilities of achieving stress reduction in materials in high aspect ratio parts. The project will investigate the practical implementation of torsional stress relief and strive to obtain results proving the feasibility. Results will be compared to what is achievable with classical lateral (flexural) vibration stress relief.

## 3 Pre-Analysis and Literature Study

The objective of developing a new VSR-inspired system that uses torsional oscillations (twisting) to reduce residual stresses in high aspect ratio parts has been investigated by a few researchers. In some the published work and combination of the more well-known flexural vibration (VSR) and torsional vibration has been investigated. This topic is being addressed in the research community, where (Cai, 2017), among others, have investigated the effects in the use of torsional oscillations, showing a reduction in the natural frequency of a test rod from 332.39 Hz to 103.8 Hz using torsional oscillations. The results of application of

both torsional and lateral vibration show that the combination yields a higher degree of reduction in residual stresses and that applying a torsional vibration with considerable dynamic stress contribution is easier to achieve compared to lateral vibration. The research results have demonstrated reduction in residual stresses in the test specimen without having a practical outcome for the industry yet. In the literature study made by Cai, some similar results were reported by other researchers on parts with geometries resembling axles and flywheels.

In (A S M Y Munsif, 2001) investigations on three types of welded shafts showed redistribution of stresses in two cases and significant reduction in stresses in one case. The stress magnitude and distribution in the parts before torsional destressing appear to influence the success rate of the process, spot welded specimen yielding best results. Spot welds generate very localized and inhomogeneous stress build up. I.e., bars, rods, shaft or axles with inhomogeneous stress build-up are relevant candidates for successful treatment.

## 4 Hypothesis

The idea is to develop a new VSR-inspired system that uses torsional oscillations (twisting) to reduce residual stresses in rod materials instead of the previous vibration superposition of structures or flexural vibration of structures.

This hypothesis is being addressed in the research community, where Cai et al. (2017), among others, have investigated the effects in the use of torsional oscillations, where their results show a reduction in the natural frequency of a test rod using torsional oscillations. The research results have demonstrated efficacy without having a practical outcome for the industry yet.

## 5 Success Criteria

- Documented change in material stress in rods from min. 2 case companies either from Pre/post scan on frequencies (performed at DAMRC) or by perceived experience when machining (by companies)
- Organizing of at least one event with external stakeholders interested in the deployment of the technology before project ends.

## 6 Project Scope

This pre-project aims to create a solid proof-of-concept, where methodology and technology are tested on business cases, after which the insights are disseminated to interested companies, who in subsequent development project(s) will mature and commercialize the technology for the benefit of several different industry segments e.g. energy, automotive.

## 7 Risk Analysis

DAMRC has no prior experience with torsional oscillations of material for which reason iterations of prototypes to reach a functionable test setup must be expected. To cope with this uncertainty 20% of the total project hours has been set for construction and initial testing of the test setup.

There is an assumption that changes in frequencies within the rod material can be detected by DAMRC available pre/post scanning equipment used to VSR treatment today. If this is not the case other ways to detect changes will be to explore DAMRCs existing equipment such as TapTest accelerometer or SpinScope software. Another way to analyze the effects of TORSR treatment, will be the experience from the case companies when machining with the treated and non-treated material.

## 8 Experiment Design

The overall purpose of the experiment design is to qualify if torsional stress relief treatment offers new possibilities. To this end, a torsional test set-up will be designed and realised and in parallel a VSR test set-up capable of treatment of same test specimen. Cylindrical steel bars of different lengths and diameters have been selected for testing. The rationale behind choosing cylindrical bars for test specimen are four-fold,

- these bars are used widely in industry,
- they are typically cold drawn and therefore have stresses,
- they are easy to acquire,
- and we can order them in an industrially relevant dimension which is manageable in terms of suitable test equipment and handling of the rods.

Two different diameters,  $\varnothing 25$  mm &  $\varnothing 50$  mm, and three lengths app. 1500 mm, 3000 mm and 600 mm ( $\varnothing 50$ ). In this way effects of different diameters and aspect ratios can be tested.

To demonstrate the feasibility of torsional stress relief a series of tests have been conducted on bars in various states,

- torsional treatment of "as delivered bars" (cold drawn and hence with residual stresses),
- bars that have been stress relieved and restressed thermally and mechanically,
- for reference and comparison, several bars have been subjected to normal flexural VSR treatment,
- and some bars have not been subjected to treatment at all.

The  $\varnothing 25$  bars have been delivered as 3000 mm bars and will tested as such. After testing they will be cut in half and tested as 1500 mm bars. The bars are tested in a dedicated test set-up where torsional vibration can be induced with variable torque and frequency through application of a vibrator and an accelerometer used as motion sensor for monitoring of torsion frequency.

## 9 Experimental Procedure

The overall procedure for demonstrating torsional stress relief is to document the state of the test specimen before starting treatment and compare to the state after treatment. Since we cannot measure the amount of stress in a part directly, we focus on measuring the change from before treatment to after treatment. The Metalmax taptest equipment have the capability to detect resonance (Eigen) frequencies in

a part, which is known to be linked to the residual stress state of a part. A change in resonance frequencies thus indicates a change in stress state all else being equal. The procedure for testing is therefore,

1. Taptesting
2. Inducing stresses in the specimen, thermally or mechanically
3. Taptesting to ascertain residual stresses in the specimen
4. Torsional/flexural stress relief treatment
5. Taptesting to qualify residual stress reduction

## 9.1 Natural frequencies versus residual stress

In physics, it is an accepted fact that natural frequencies of a component are a product of mass and stiffness. This project makes use of the general assumption that residual stresses in a component typically increases the stiffness and thereby also the natural frequency. This is common for most steel materials. Since DAMRC already is in possession of equipment, capable of measuring natural frequencies in a component (Metalmax) and due to that, methods for measuring stresses directly is limited to measuring outermost layers of material and is very costly, it has been decided to test the capability of the Metalmax system for the purpose of indirect stress measurement in this project. The Metalmax is a system for taptesting machining tools but is basically a tool for measuring natural frequencies also.

## 10 Design of test set-up

For the design of a test set-up of the three different bar sizes, some preparative actions have been made. The  $\varnothing 50$  mm bar is the first one to be tested. To determine if the planned test set-up will be able to match the needed torque to reach a level close to yielding in the material, a FEM analysis have been a long with a test of the performance of the vibrator intended for the test.

The resulting test set-up for torsional vibration is depicted on figure 1.

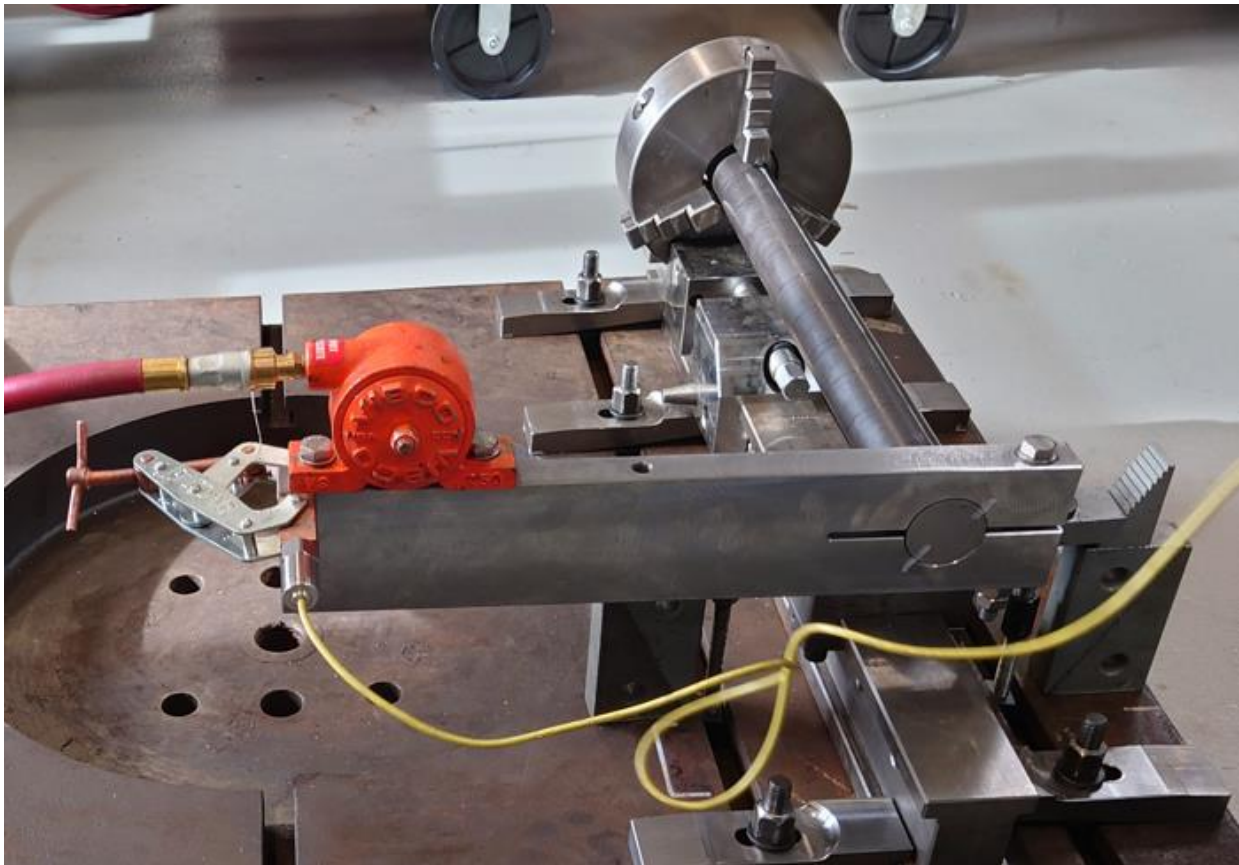


Figure 1: Test set-up for torsional vibration treatment of bars.

The orange vibrator is mounted on a torsion arm clamped onto the bar to be treated. An accelerometer for detection of the vibrations is located at the end of the yellow wire. The test object mounted on this picture is the  $\varnothing 50$  mm bar. The bar is fixed in the far end to obtain the needed torque. This treatment set-up is used for all the tests, though in some tests another vibrator is applied.

The pneumatically driven orange vibrator is tested to obtain a characteristic of the G acceleration as a function of rpm. This info is used for checking stresses in a FEM simulation of the test set-up to ensure sufficiently large torque on the bar in the treatment process, please see following sections for details.

Based on the result of the test and the FEM simulation, it was determined that considering all the assumptions made, the creep in the material will be achieved at RPM values close to the natural frequency of the system  $56,695 \text{ Hz} \Rightarrow 3396 \text{ RPM}$  before reaching any elastic limit due to the value of a static force. In the further testing with use of the pneumatically driven vibrator the RPM is set by rpm measurement through the accelerometer.

## 10.1 NATURAL FREQUENCY OF THE SYSTEM.

The geometry of the system for which it is sought to obtain natural frequency is composed of a rod fixed at one of its ends and supported by a bearing that constrains all rotation and displacement in different directions than the axis of the rod. At the other end, the rod is attached to a beam through which the system is driven by an unbalanced air turbine motor. The geometry is shown in Figure 1

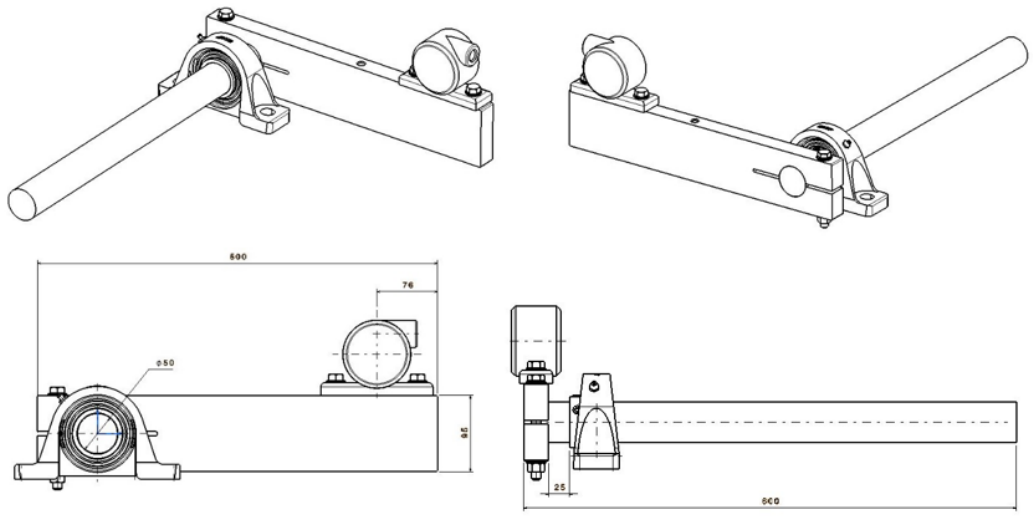
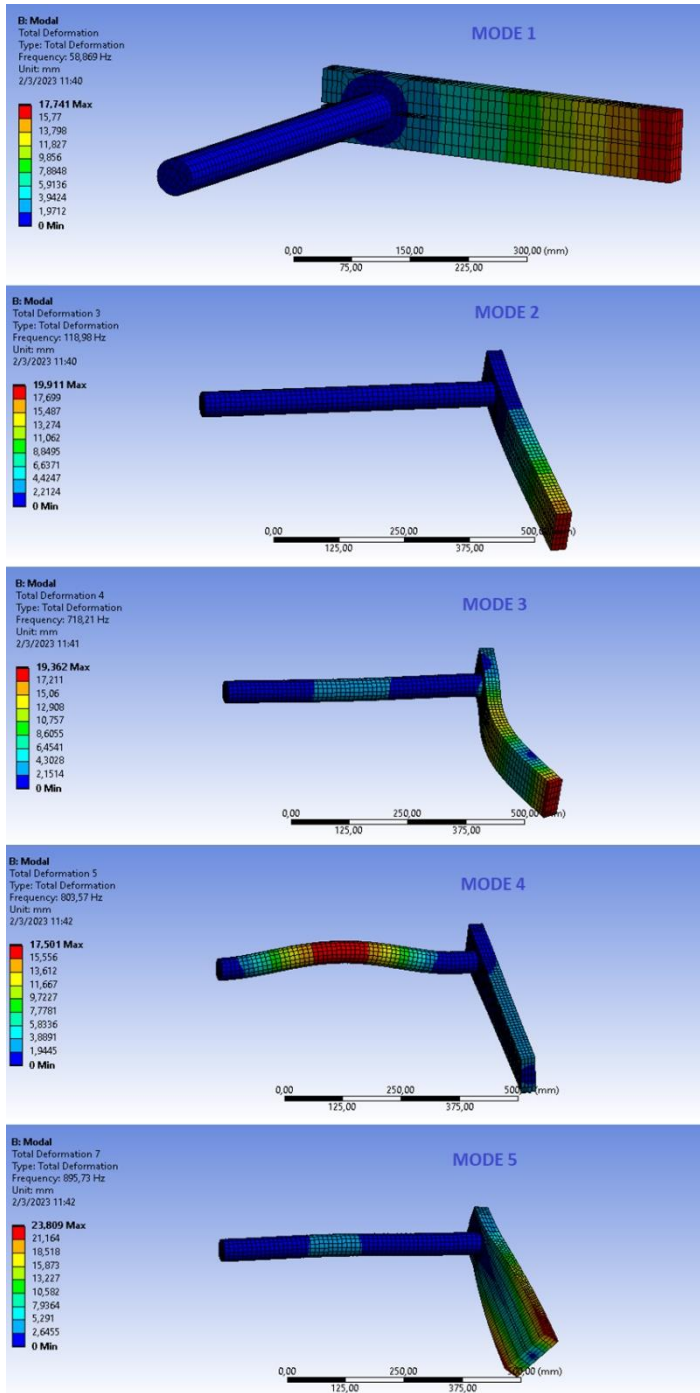


Figure 2: Geometry of the system.

To get the natural frequencies of the system, this geometry was pre-processed and analyzed with FEM. A modal analysis is made for this model where the natural frequencies are obtained and shown in Table 1. Each of these modes of vibration are associated with different configurations of deformation in the system and this can be seen in Figure 3. It is important to mention that although all these modes can be excited by high-frequency harmonics resulting from system dynamics, obtaining modes higher than the first mode are mostly theoretical because the components are more likely to fail before having one of these modes in pure resonance. That is why we consider our natural frequency only as the value corresponding to the first mode of vibration, 58.9Hz.



Mode of vibration	Frequency (Hz)
1	58,869
2	118,98
3	718,21
4	803,57
5	807,73
6	895,73

Table 1: Natural frequencies

Figure 4: Modes of vibration

## 10.2 PNEUMATIC TURBINE MOTOR VS-250 – FORCE AND RPM ANALYSIS.

For the purpose of being able to predict the behavior of the pneumatic motor VS-250 in different ranges of RPM to be able to adjust the output to match the yield stress in the bar, a test to measure the vibration force exerted by the motor is made.

The pneumatic motor is fitted to a part with a much greater mass and rigid structure to avoid the effect of externals system in the vibration measurement (All the vibration will be absorbed by the pieces with less rigidize, the structure of the motor). Then an accelerometer is connected to the support of the motor as the more near position available to take measurement (the device to fit the accelerometer doesn't have the width necessary to fit the accelerometer directly in the motor and the magnetic fixture of the accelerometer to fit it directly in the case of the motor is not available). After that, the pneumatic motor is connected to a device composed by three air valves, one mater valve and others two derived than the last one to drive two motors in separately way, see Figure 5. To set the test, considering that only one motor is used, the master valve is open at 100%, the other individual valve which any connection is close at 0% and the other individual valve where the motor is connected is used to change the RPM of the motor, whereby different open rates are used with this valve to get different values of RPM during the measurements. Starting with the valve nearly closed, three different g-force and RPM measurements are taken at the same air valve position, then progressively opened and three measurements are taken for all different valve positions between 0% and 100% of the opening.



Figure 6: Pneumatic motor - Vibration analysis.



Figure 5: Air valves device.

These sets of values return a table with different g-force values associated with the corresponding RPM value, see Table 2. In order to clean up all the information, this table is reorganized by placing the different RPM values from lowest to highest and taken an average of the g-force for the same RPM values in different measurements. See table 3.

Although the absolute value of each of these measurements is not relevant for our purpose, we understand that the relationship between the different values is directly associated with the force values induced by the unbalanced mass of the pneumatic turbine rotor. Considering that, we can give weight to the relative value between the different values of g force to derive a scaled function of the force exerted by the turbine with known data from the data sheet of this, and that has the same variation of the force g obtained in the different measurements. With this perspective, the values are taken and an evaluation of the best regression model to make a description of the behavior of the data is analyzed.

For the case study, the exponential regression model have a better description of the data based on the highest values of the R2 factor (Index that shows us how well the values s are represented by the function), see Figure 7.

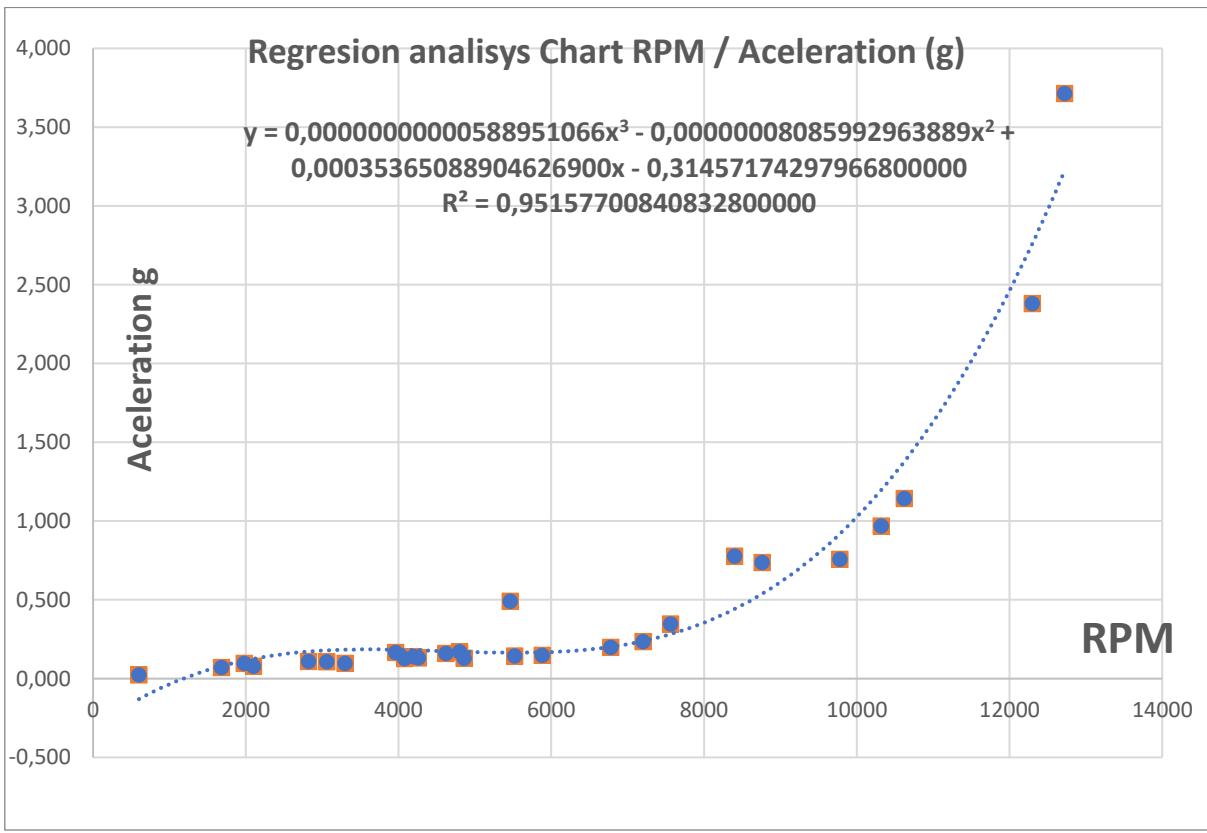


Figure 7: Polynomic regression model.

If we consider the fact that we are interested in an RPM range close to the natural frequency of the First vibration mode (58.869 Hz = 3532 RPM) , the exponential regression model is the one that has a better representation of our area of interest. So, it's possible to say that the g force is represented by:

$$g = 0,032670 \cdot e^{0,00034 \cdot RPM}$$

Considering the fact that the force F applied by the pneumatic turbine is proportional to the acceleration perceived, we can write:

$$F = g \cdot A$$

With A like a constant.

$$F = A \cdot 0,032670 \cdot e^{0,00034 \cdot RPM}$$

Then we know from the data sheet of the pneumatic turbine than for 7200RPM we have 2225N of force applied, so:

$$2225N = A \cdot 0,032670 \cdot e^{0,00034 \cdot (7200)}$$

From where:

$$A = \frac{2225N}{0,032670 \cdot e^{(0,00034 \cdot (7200))}} = 5888,81$$

Then:

$$F = 192,38 \cdot e^{0,00034 \cdot RPM}$$

Considering that our objective is achieve the yield fluence stress in the surface of the circular rod we can write in base of the elastic theory for the Shear Stress:

$$\tau = \frac{M_t \cdot r}{I_p}$$

Where  $\tau = \text{Shear Stress}$  ,  $M_t = \text{torsor moment}$  ,  $r = \text{radius of the rod}$  and  $I_p = \text{polar inercial moment of the rod section}$ . Then:

$$M_t = \frac{\tau \cdot I_p}{r}$$

Now we have different forms of evaluation and one of them is to consider a force with the capacity to generate an elastic limit in the material without considering the dynamic effect, that is, considering a force with the necessary value to achieve creep. To obtain this value we can substitute the formulation of our force in the moment formula, where l is the lever arm (distance between the axe of the rod and the center of the motor):

$$l \cdot F = \frac{\tau \cdot I_p}{r}$$

$$l \cdot 192,38 \cdot e^{0,00034 \cdot RPM} = \frac{\tau \cdot I_p}{r}$$

If we are interested in obtaining the theoretical RPM at which the motor will give us a force with the necessary value to obtain the elastic limit in the material, we can write:

$$e^{0,00034 \cdot RPM} = \frac{\tau \cdot I_p}{192,38 \cdot l \cdot r}$$

$$0,00034 \cdot RPM = \ln \left( \frac{\tau \cdot I_p}{192,38 \cdot l \cdot r} \right)$$

$$RPM = \frac{\ln \left( \frac{\tau \cdot I_p}{192,38 \cdot l \cdot r} \right)}{0,00034}$$

From the Mohr circle theory, we know that.

$$\tau_y = \frac{\sigma_y}{2}$$

And also for e circular section of the rod:

$$I_p = \frac{\pi \cdot d^4}{32}$$

$$RPM = \frac{\ln\left(\frac{\frac{\sigma_y}{2} \cdot \frac{\pi \cdot d^4}{32}}{192,38 \cdot l \cdot r}\right)}{0,00034}$$

Considering  $\sigma_y = 250Mpa$  ,  $r = 0,025mm$  and  $l = 0,349mm$

$$RPM = \frac{\ln\left(\frac{\frac{250Mpa}{2} \cdot \frac{\pi \cdot 0,025^4}{32}}{192,38 \cdot 0,349 \cdot 0,025}\right)}{0,00034} = 5124,9RPM = 85Hz$$

Where we could see that the RPM necessary to obtain the elastic limit in the material is greater than the RPM necessary to obtain the natural frequency of the system in the first mode of vibration. So, the next step is to analyze if in the RPM the natural frequency of the system, we can achieve the elastic limit in the material by the formulation obtained based on the force induced by the engine. To do that, we built a table with different values of the Force for different values of RPM obtained across our formulation, to then input these values of a dynamics simulation of the system:

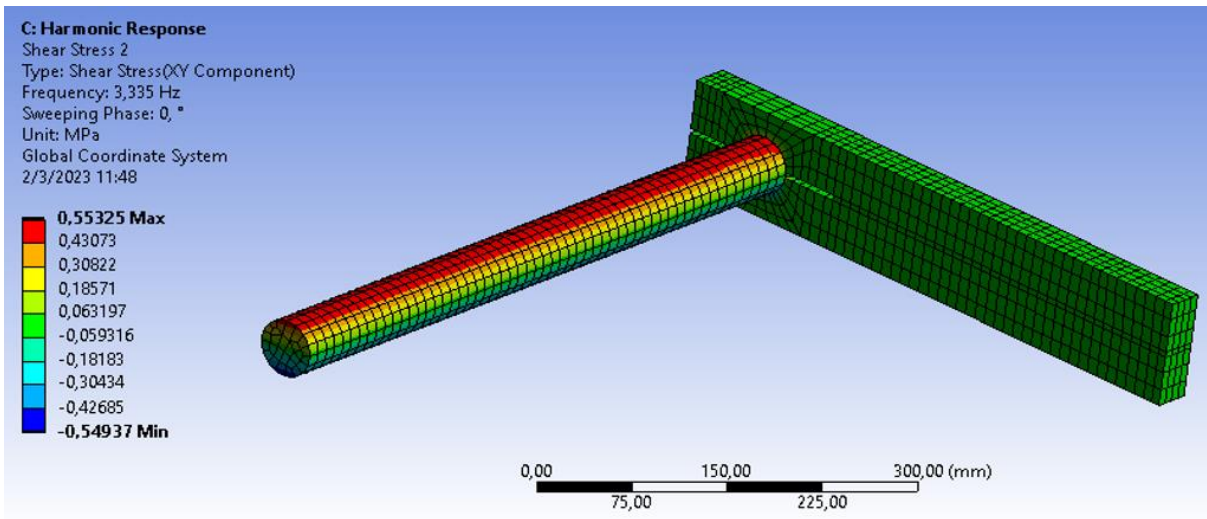
RPM	Hz	Force (N)
2100	35,0	392,9
2200	36,7	406,5
2300	38,3	420,5
2400	40,0	435,1
2500	41,7	450,1
2600	43,3	465,7
2700	45,0	481,8
2800	46,7	498,5
2900	48,3	515,7
3000	50,0	533,5
3100	51,7	552,0
3200	53,3	571,1
3300	55,0	590,8
3400	56,7	611,3
3500	58,3	632,4
3600	60,0	654,3
3700	61,7	676,9
3800	63,3	700,3
3900	65,0	724,5
4000	66,7	749,6

Table 5 – Force Values – RPM Pneumatic motor

Making a F.E.M simulation with the different values of force for each value of RPM, the result showed in the table 7 are obtained:

ITERATION	FRECUENCY (Hz)	YIELD SHEAR STRESS (Mpa)	RPPM
1	3,335	0,55325	200,1
2	6,67	1,1173	400,2
3	10,005	1,7036	600,3
4	13,34	2,3253	800,4
5	16,675	2,9979	1000,5
6	20,01	3,7411	1200,6
7	23,345	4,5807	1400,7
8	26,68	5,5523	1600,8
9	30,015	6,7068	1800,9
10	33,35	8,1212	2001
11	36,685	9,7868	2201,1
12	40,02	11,921	2401,2
13	43,355	15,008	2601,3
14	46,69	19,792	2801,4
15	50,025	28,296	3001,5
16	53,36	47,249	3201,6
17	56,695	124,23	3401,7
18	57	145,08	3420
19	60,03	240,3	3601,8
20	63,365	64,668	3801,9
21	66,7	38,636	4002

Table 7 – Result of F.E.M dynamics simulation.



Based on the result of the test and simulation, it is possible to observe that considering all the assumptions made, the creep in the material will be achieved at RPM values close to the natural frequency of the system  $56,695 = 3396\text{RPM} \rightarrow \tau_y = \frac{\sigma_y}{2} = 125\text{Mpa}$  before reaching any elastic limit due to the value of a static force.

The test set-up used for  $\varnothing 25$  mm bars is similar to the set-up for the  $\varnothing 50$  bar set-up, please figure 2. The difference is that the pneumatical vibrator is replaced with an electrical one from our VSR system and then also controlled from the VSR controller which means that we have better control of rpm setting and also optional documentation of the rpm control during the test.



Figure 8,  $\varnothing 25$  mm bar test set-up. Silver VSR vibrator mounted on torsional arm. Bar is fixed in one end and supported with a bearing in the other end. This set-up is used both for app. 3000 mm bar and app. 1500 mm bar. The vibrator is balanced vertically to eliminate static load and hereby also overload of the bar.

### 10.3 Flexural (VSR) treatment set-up.

A set-up was made for flexural vibration of bars for reference. Flexural vibration is the closest competitor to ToRSR. As seen on the picture of the set-up the bar is clamped in one end onto the vibration table and simply supporter app. One third of the length to ensure proper magnitude of the acceleration (G) in the bar.

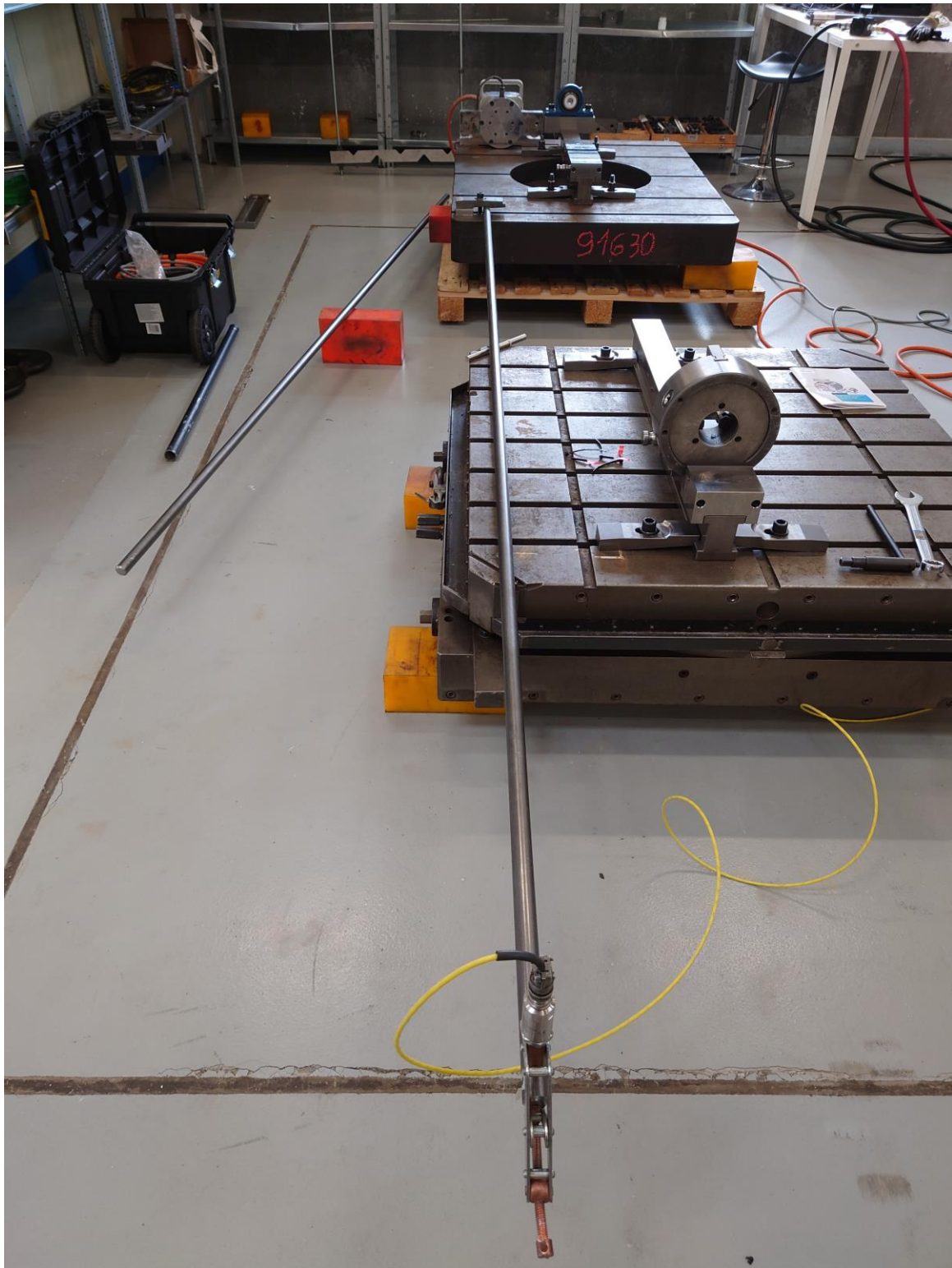


Figure 9: flexural vibration set-up. The bar is supported 2/3 from the end.

#### 10.4 Re-stressing of de-stressed bars

To build up stresses again after relaxing the  $\varnothing 50$  mm bar, a propane gas flame was applied locally on the bar for inhomogeneous heating and succeeding rapid cooling with cold water for 20 minutes, since this normally induces warping and stresses in a part. After the rapid cooling a small warping was detectable when rolling the bar on a flat surface.

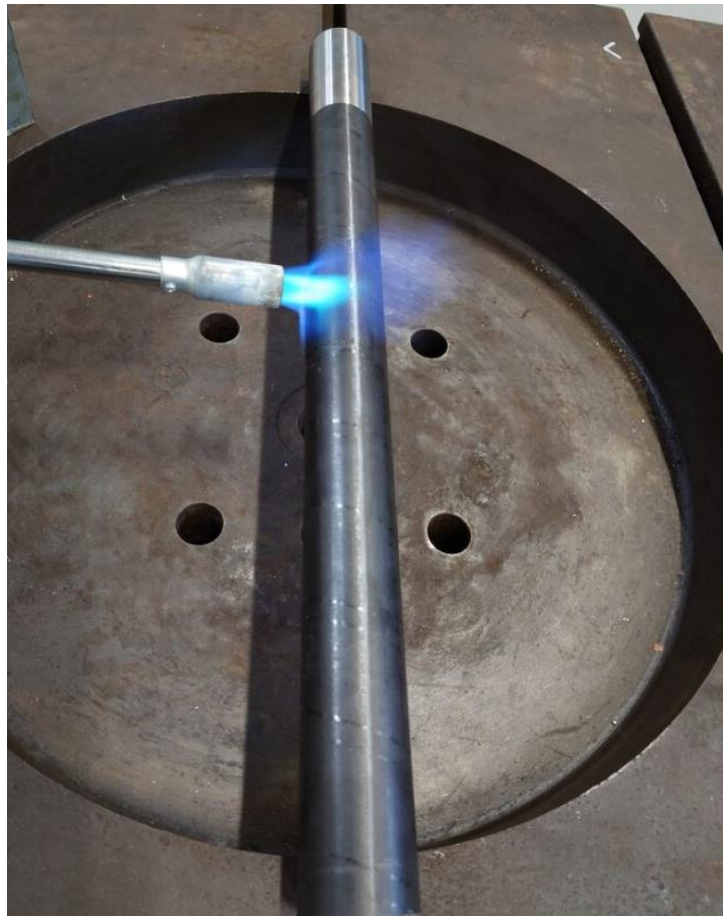


Figure 10: thermal stressing of bar with propane gas flame

The  $\varnothing 25$  mm long bars were re-stressed by local bending of the bars until they showed permanent deflection, thereby ensuring some level of residual stresses. Figure 5 illustrates the small deflection after bending.



Figure 11: demonstration of the small deflection after bending.

## 10.5 Taptesting

While developing torsional stress relief technology a need to gauge the effectiveness of the treatment is identified due to the difficulty involved in measuring residual stress.

To this end, a series of tap tests was conducted on the test specimen used during the initial TorSR experiment.

## 10.6 Introduction

Having constructed an experimental setup to test the effects of TorSR, there remains a need to be able to consistently and reliably measure changes in the frequency response function (FRF) of the test specimen (the rod subjected to torsion) to gauge the effectiveness of the treatment. For this reason, tap tests are performed on the test specimen and experimental set-up. Following an initial experiment involving TorSR treatment and pre- and -post treatment tap tests of the test specimen and experiment setup; additional tap tests be performed with the aim of demonstrating the repeatability of the tap test procedure.

The purpose of this section is to present the methodology and results of the tap tests.

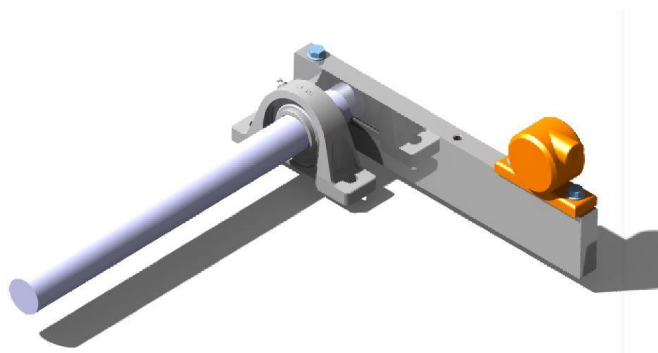


Figure 1: 3D rendering of the experimental setup. Note that in the experiment the end of the rod opposite the torsion bar has a fixed boundary condition.



Figure 2: Placement of the test specimen during tap tests when removed from the experimental set-up.

Data from the tap tests were obtained using MetalMax TXF software and analysed in Microsoft Excel. Interim results of the initial tap tests (meaning before the analysis was completed) were presented to project engineers and are reproduced in Figure 3 to Figure 6 for convenience. After a debrief of the TorSR

experiment and a review of the tap test data, it was decided that additional tap tests be performed to a) assist in interpreting the initial results, including determining the root-cause of the change in FRF and b) demonstrate the repeatability of results obtained from tap tests. The methods and results of these additional tap tests are presented in the succeeding sections.

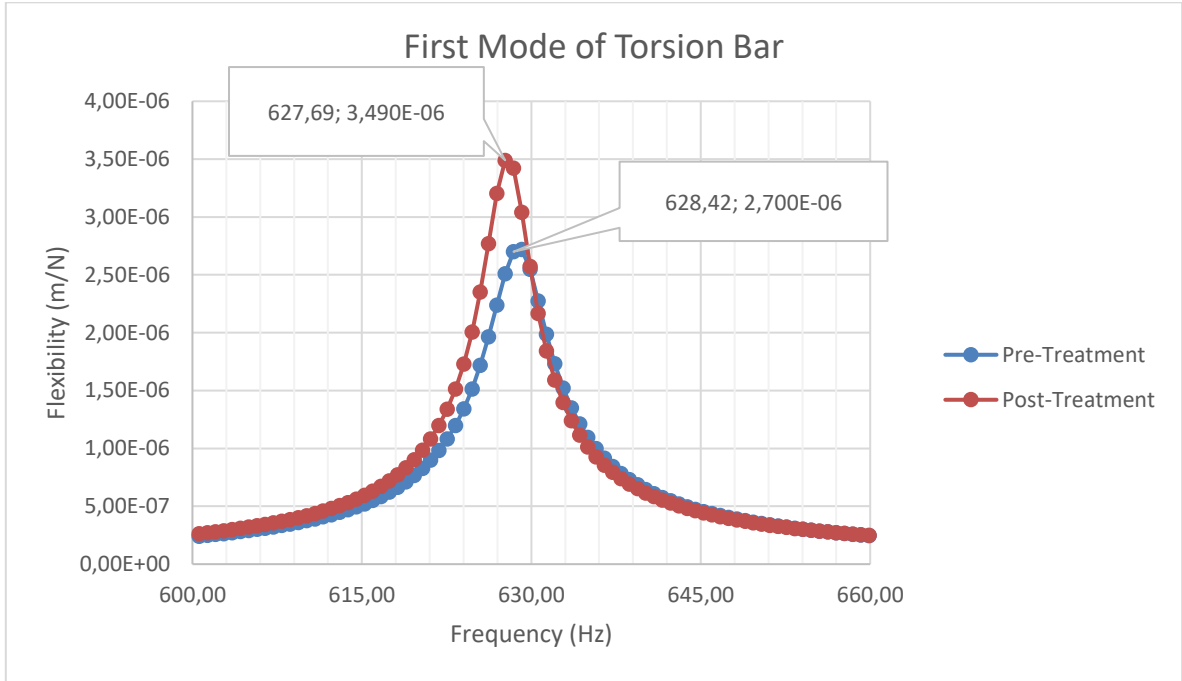


Figure 3: Comparison of the first identified mode of the Torsion bar before and after treatment. There are minor cosmetic and formatting changes to this, and the following graphs compared to the interim results presented previously.

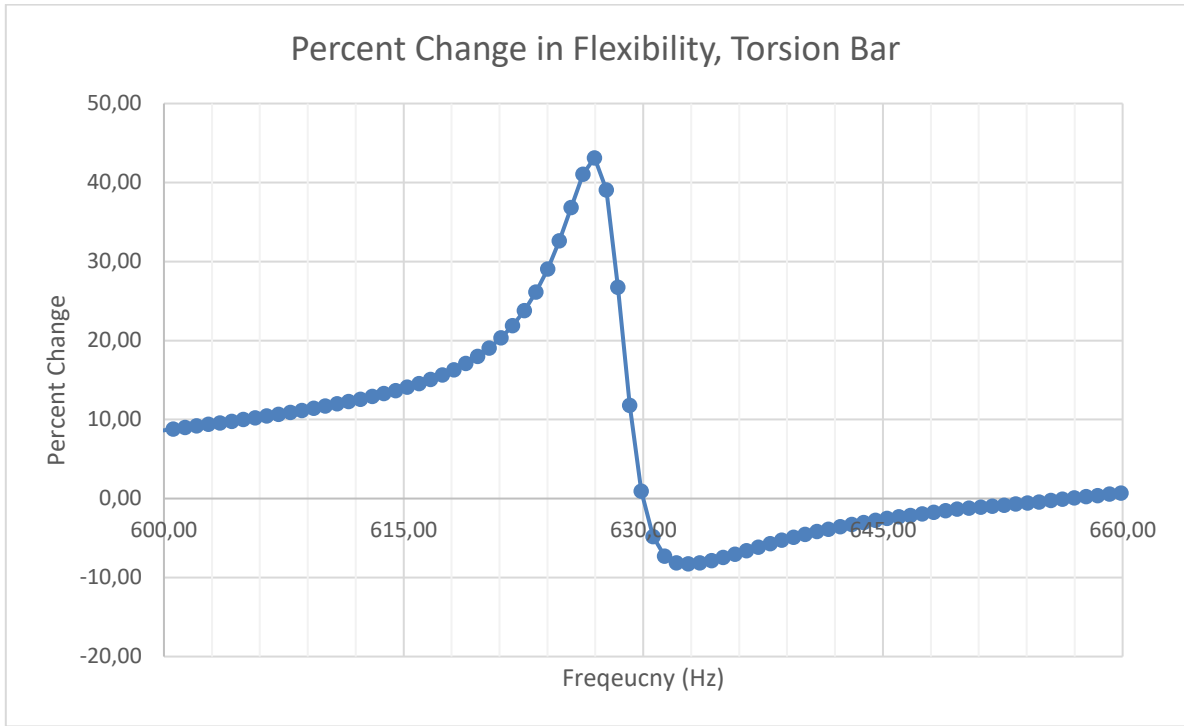


Figure 4: Percent change in the magnitude response of the FRFs in the previous graph.

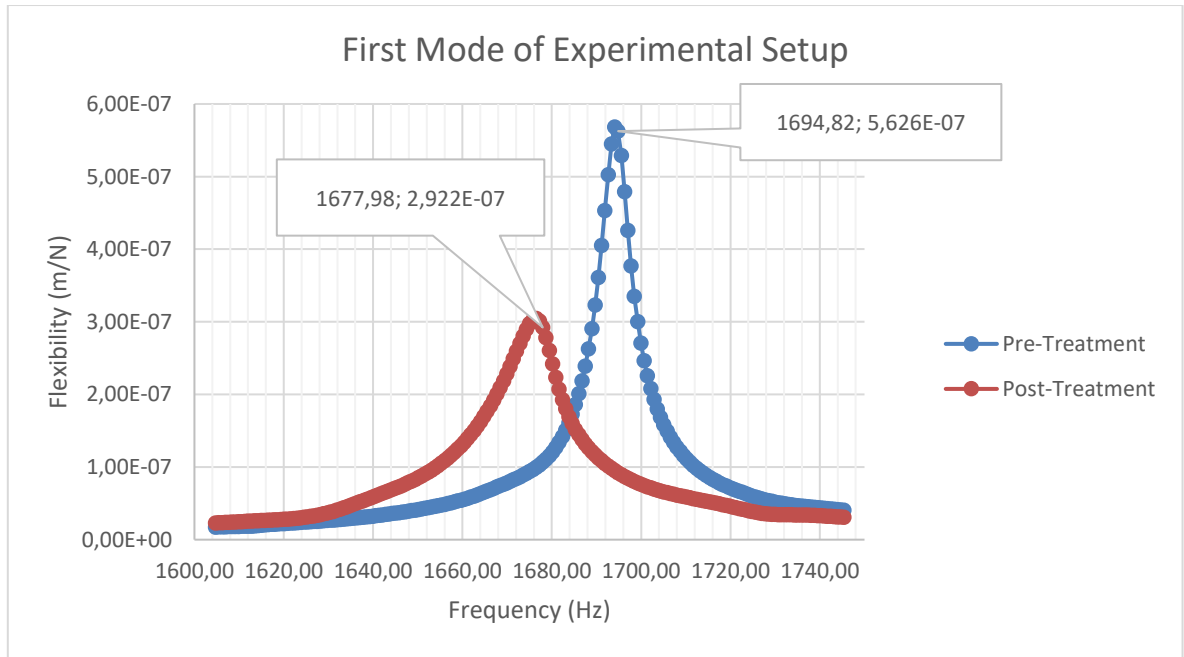


Figure 5: Comparison of the first identified mode of the experimental set up before and after treatment.

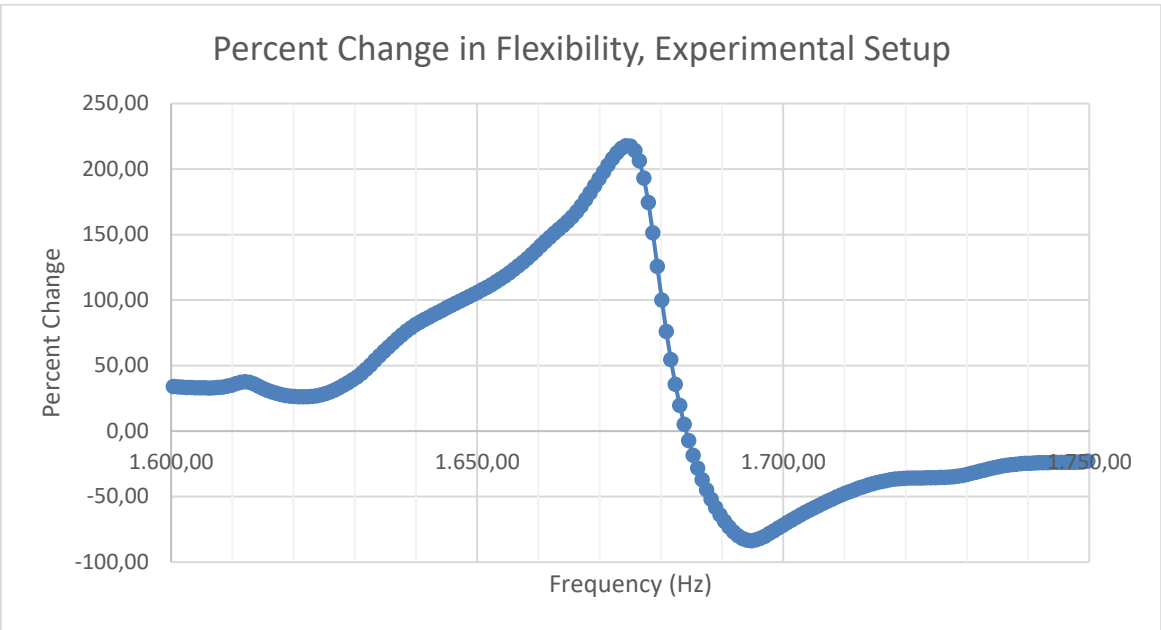


Figure 6: Percent change in the magnitude response of the FRFs in the previous graph.

### 10.7 Methodology

To demonstrate the repeatability of the results obtained from the tap test procedure, successive tap tests were performed on the torsion bar in a configuration similar to that shown in Figure 2. In lieu of making new markings of the impact locations on the test specimen, the placement of the accelerometer and impact locations are pinpointed using existing marks made during the previous experiment and also by characteristic marks left on the part during the manufacturing process. Unlike the previous experiment, the accelerometer and point of impact are located on the same side of the test specimen, with approximately 1 to 2 cm distance between the impact point and accelerometer, as shown in Figure 7.

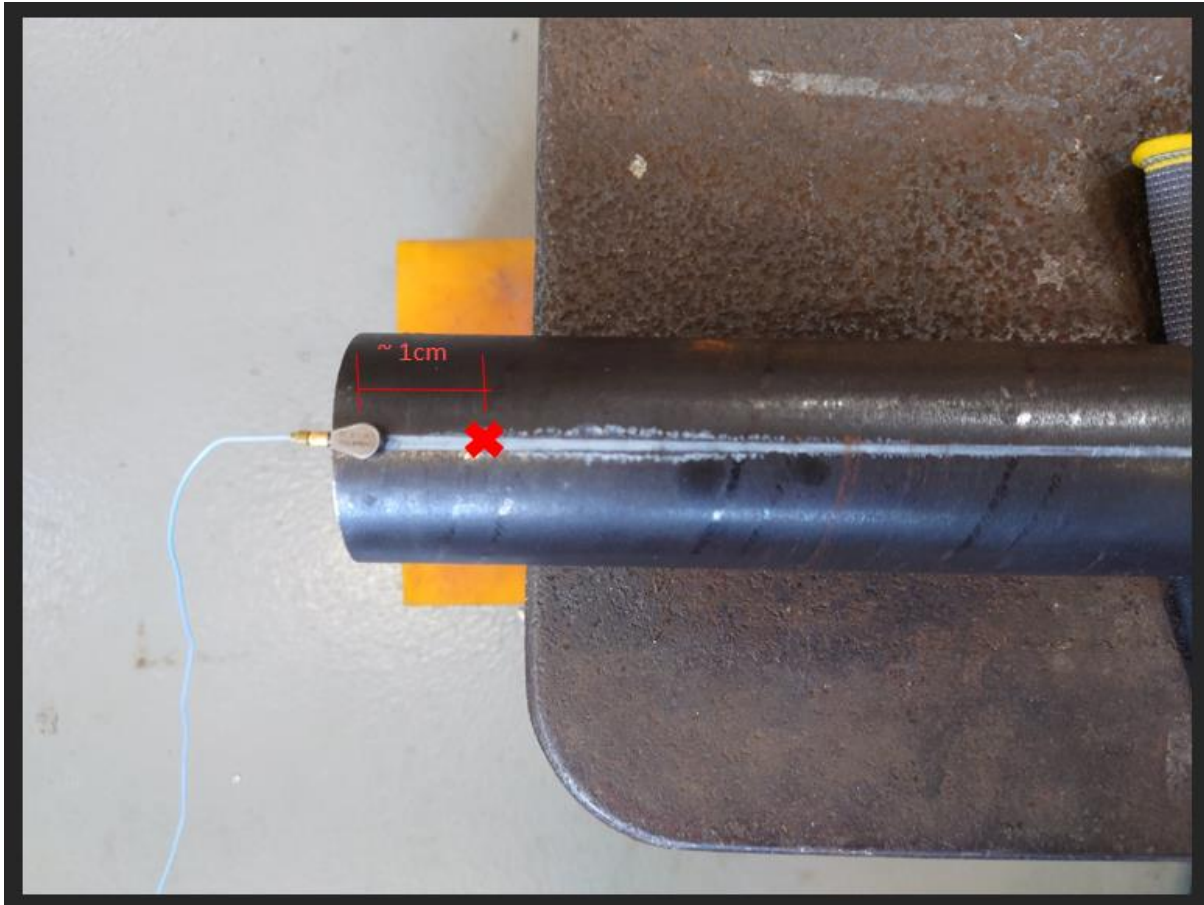


Figure 7: Accelerometer and impact location on the torsion rod. Marks made on the rod during its manufacture are used to pinpoint the location of the hammer taps.

To evaluate the repeatability of the tap test results, five tap tests are conducted using the above configuration of test specimen and transducer placement, where each tap test consists of a series of measurements obtained from hammer impacts which are then averaged by the TXF software. In this experiment, five hammer impacts are performed during each tap test for a total of twenty-five measurements. The results from each of the five tap tests are then extracted and analyzed in Microsoft Excel. For the sake of simplicity, only the first identified mode is considered in the analysis.

## 10.8 Results

The FRF of each test for the frequency band of interest is shown in **Fejl! Henvisningskilde ikke fundet.** and **Fejl! Henvisningskilde ikke fundet.**. To quantify the difference between each FRF, the data series for each resonance peak is sorted to identify the frequency at which there is a local maximum. The identified data points are then plotted in a so-called “box and whisker” graph as shown in Figure 10 and Figure 11. By visual inspection of Figure 8 to Figure 10, it is deduced that test 1 is an outlier so the plots in Figure 10 and Figure 11 are reproduced while omitting test 1. The resulting plots are shown in Figure 12 and Figure 13.

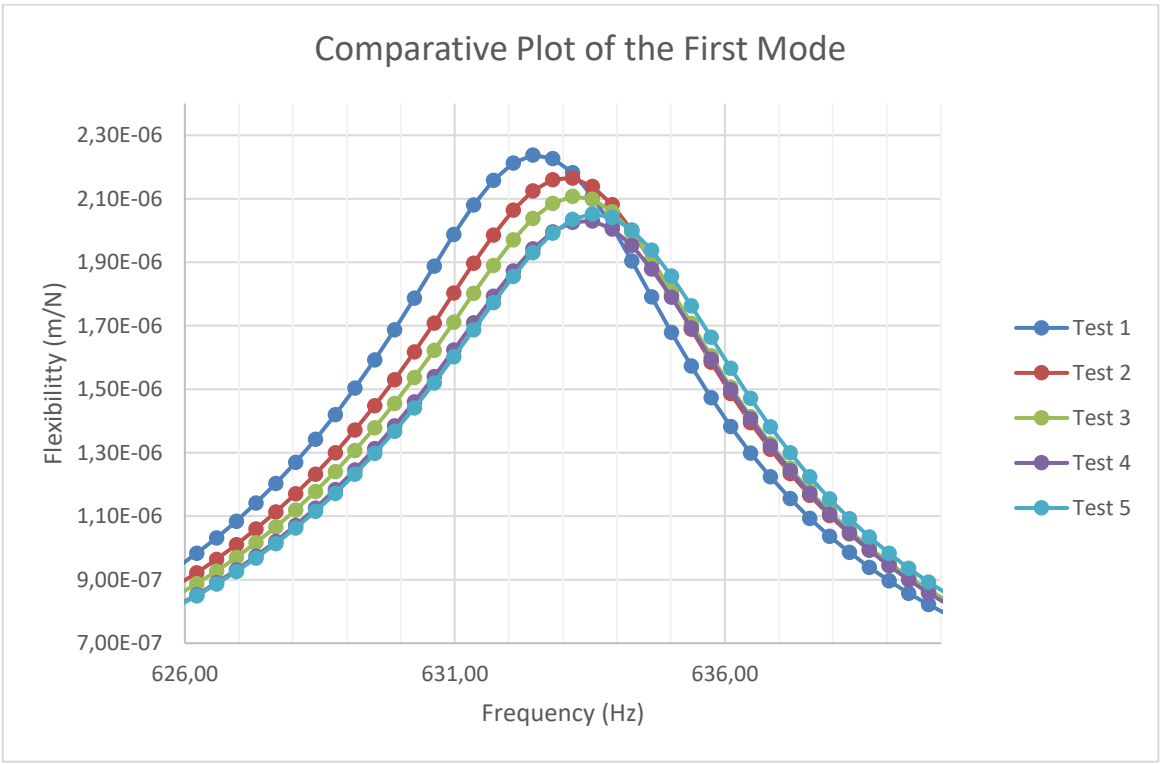


Figure 8: The resonance peak of the first mode obtained from each tap test.

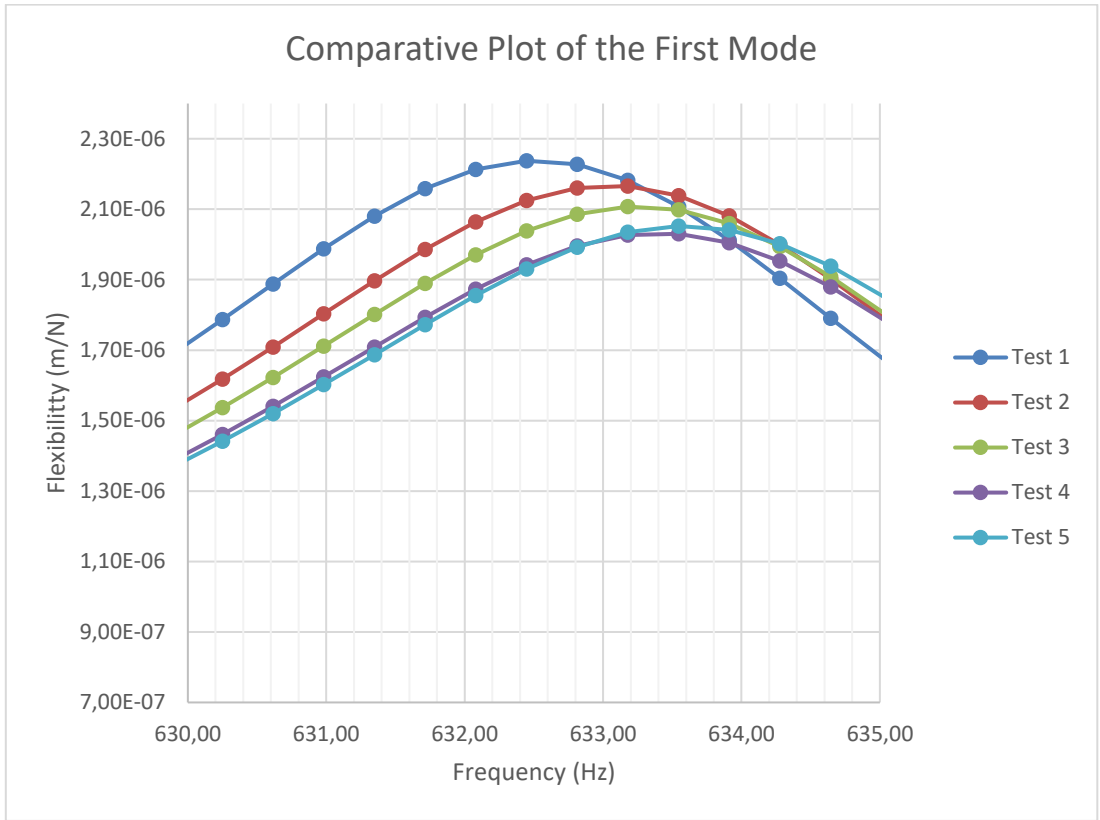


Figure 9: Detailed view of the FRFs from the previous figure.

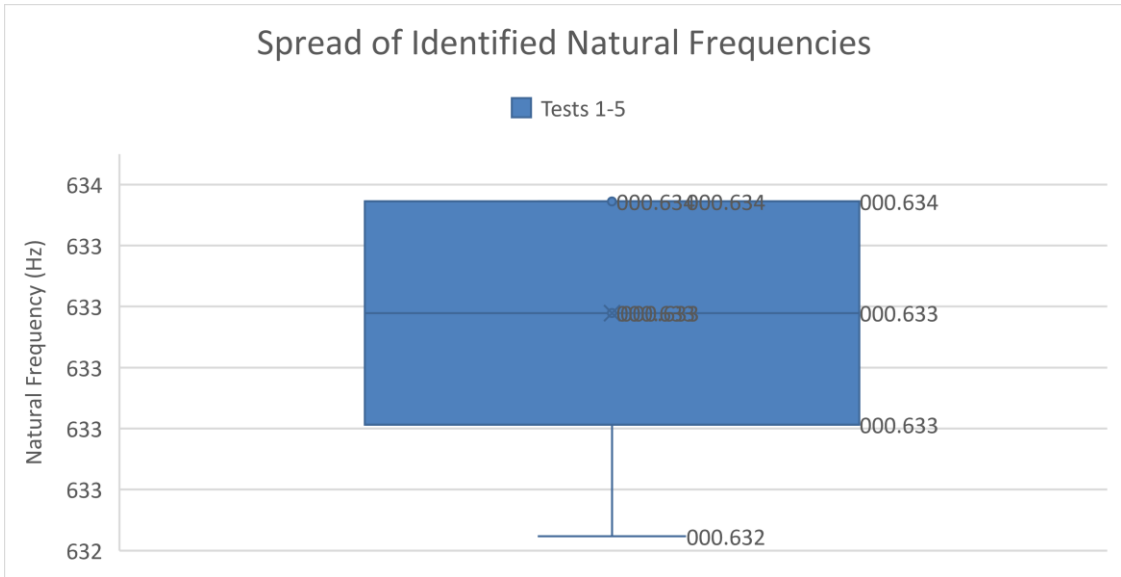


Figure 10: "Box and Whisker" plot showing the spread of the first identified natural frequency.

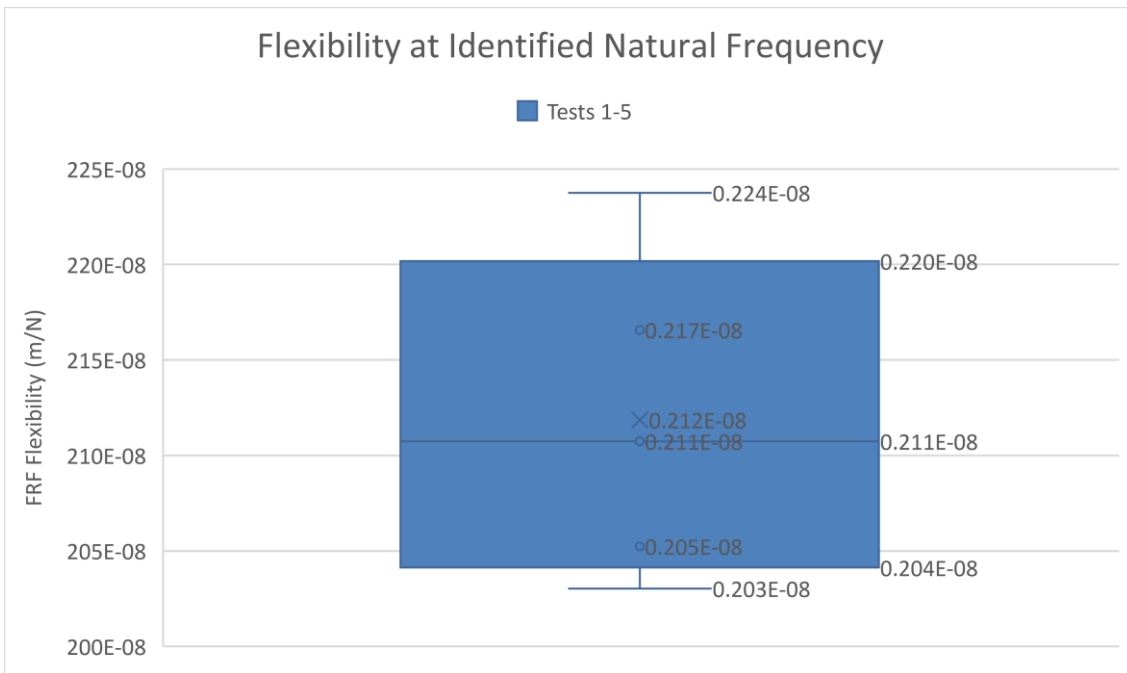


Figure 11: "Box and Whisker" plot showing the spread of the magnitude response at each identified natural frequency.

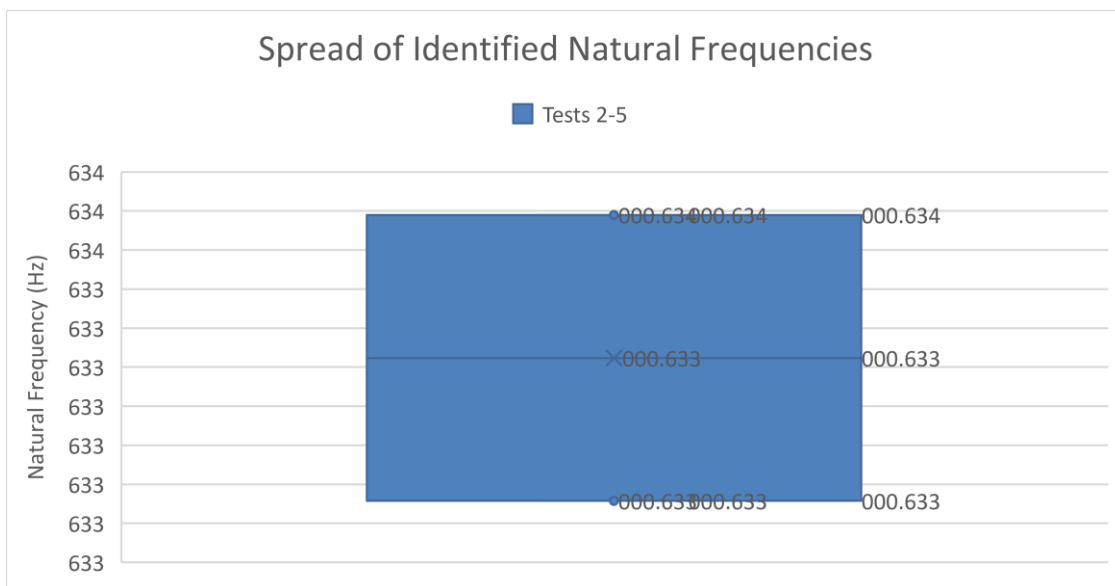


Figure 12: The spread of the identified natural frequencies is displayed with test 1 omitted.

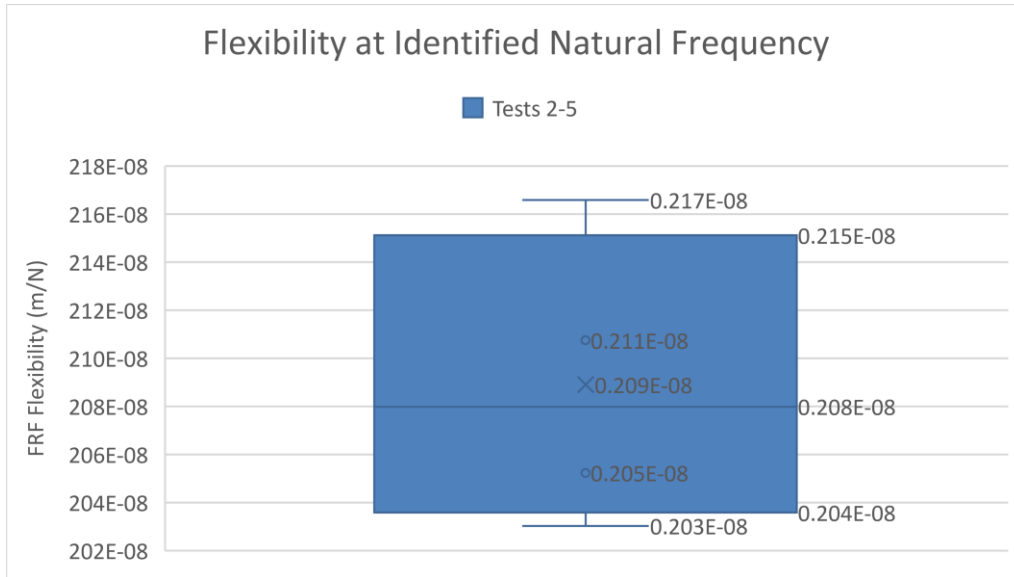


Figure 13: The spread of response magnitude at the identified natural frequencies with test 1 omitted.

Key metrics of the data presented in the above box and whisker charts are presented in Table 2 and Table 3, where the mean value is taken as the expected natural frequency or response magnitude and the Maximum Percent Difference (MPD) from the mean is calculated as

$$Max. Percent Difference = MAX \left( \frac{|Max - Mean|}{Mean}, \frac{|Min - Mean|}{Mean} \right) * 100\% \tag{1}$$

Table 2: Summary of data (identified natural frequencies) in Figure 10 and Figure 12

	<u>Max (Hz)</u>	<u>Min (Hz)</u>	<u>Mean (Hz)</u>	<u>Max - Min (Hz)</u>	<u>MPD (%)</u>
Tests 1-5	633.54	632.45	633.18	1.10	0.116
Tests 2-5	633.54	633.18	633.36	0.37	0.029

Table 3: Summary of data (flexibility at identified natural frequencies) Figure 11 and Figure 13

	<u>Max (m/N)</u>	<u>Min (m/N)</u>	<u>Mean (m/N)</u>	<u>Max - Min (m/N)</u>	<u>MPD (%)</u>
Tests 1-5	2.238E-06	2.030E-06	2.119E-06	2.073E-07	5.612
Tests 2-5	2.166E-06	2.030E-06	2.089E-06	1.355E-07	3.677

The data obtained from the tap tests conducted during the TorsSR treatment experiment is also analysed so that that data can be presented in a similar form. Sorting each respective data series to find the local maximum and performing the same calculations as before yields the results in Figure 14 to Figure 17 and Table 4 and Table 5. The results presented in this section are discussed in the next section, as are possible sources of error.

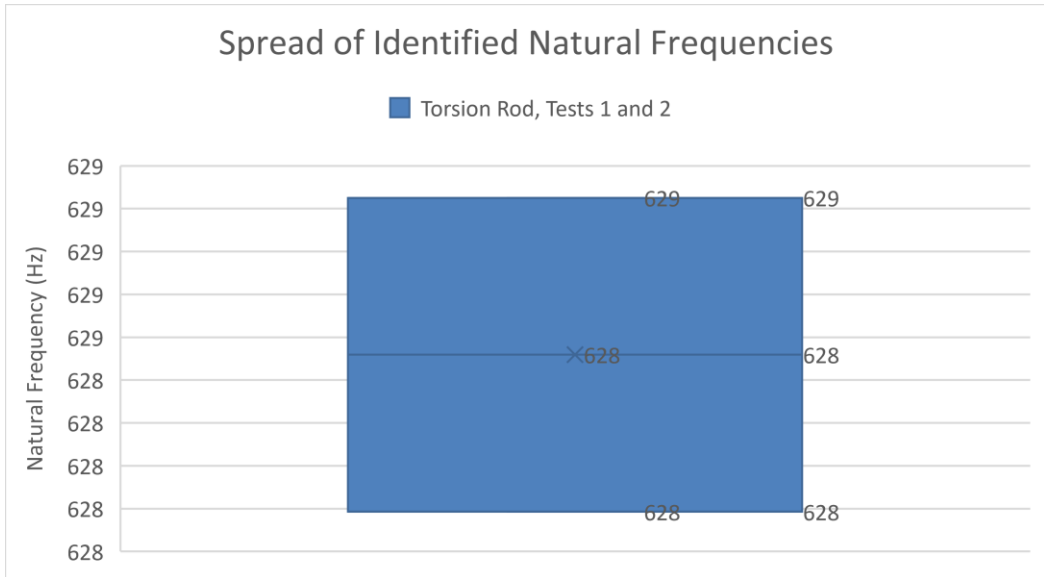


Figure 14: Box and Whisker plot of Torsion Rod natural frequencies

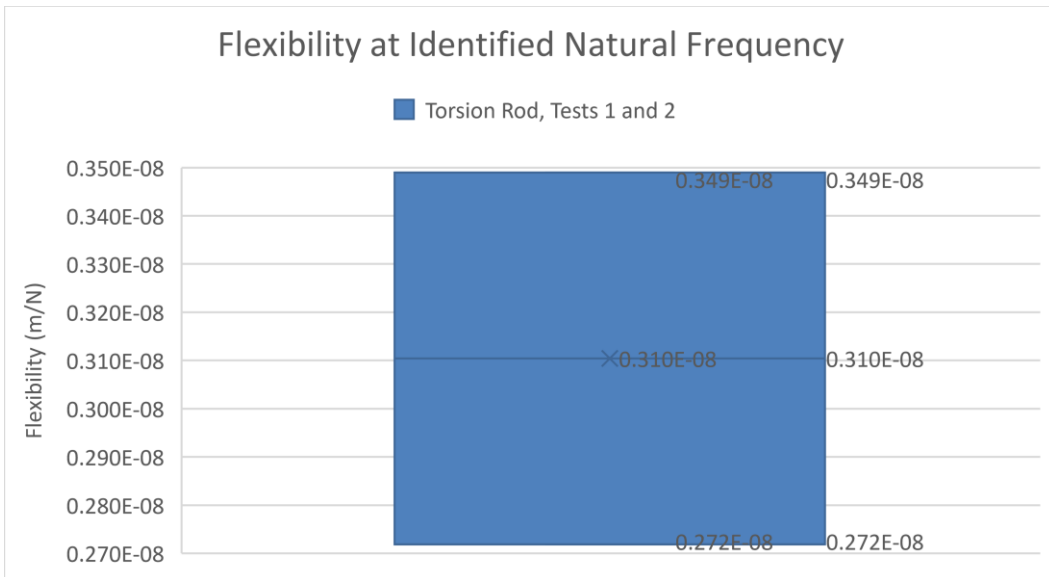


Figure 15: Box and Whisker plot of Torsion Rod Flexibilities

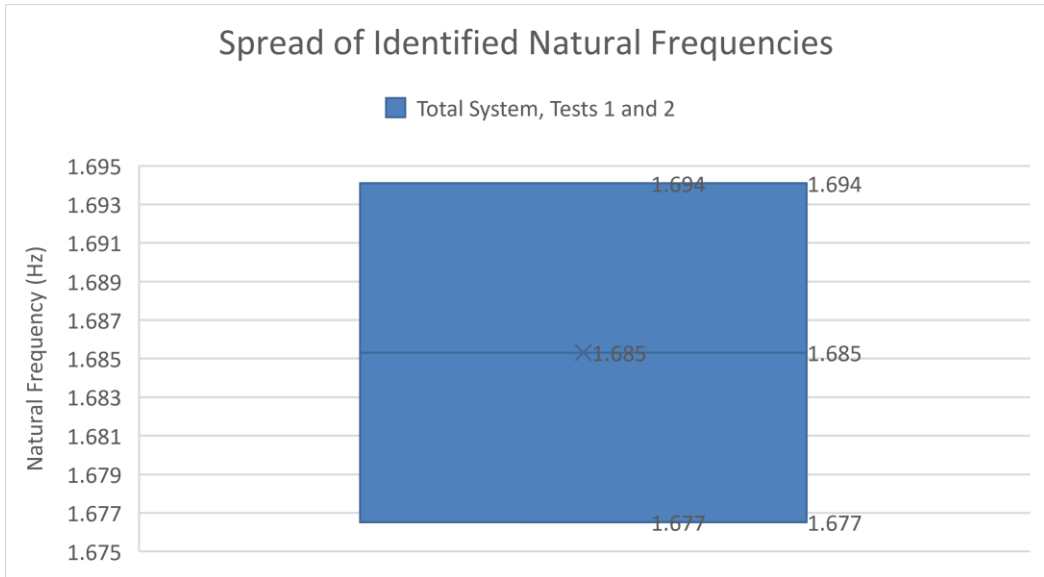


Figure 16: Box and Whisker plot of Total System natural frequencies

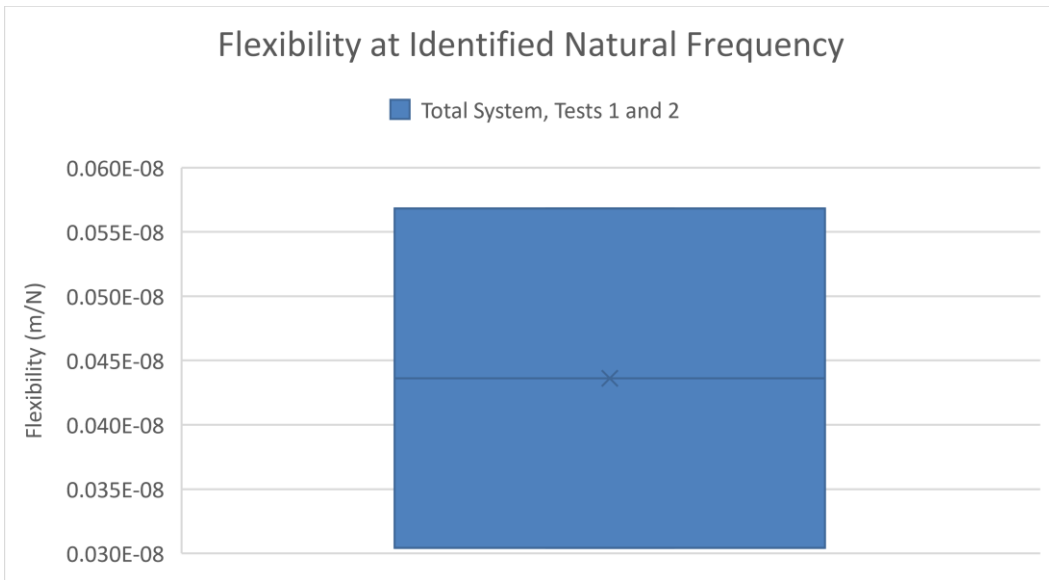


Figure 17: Box and Whisker plot of Total System flexibilities

Table 4: Key data from Figure 14 and Figure 16

	<b>Max (Hz)</b>	<b>Min (Hz)</b>	<b>Mean (Hz)</b>	<b>Max-Min (Hz)</b>	<b>MPD (%)</b>
Torsion Rod	629.15	627.69	628.42	1.46	0.116549818
Total System	1694.09	1676.51	1685.30	17.58	0.521511639
Note	For both the Torsion Rod and the Total System, max. frequency corresponds to pre-treatment and min. frequency to post-treatment.				

Table 5: Key data from Figure 15 and Figure 17

	<b>Max (m/N)</b>	<b>Min (m/N)</b>	<b>Mean (m/N)</b>	<b>Max-Min (m/N)</b>	<b>MPD (%)</b>
--	------------------	------------------	-------------------	----------------------	----------------

Torsion Rod	3.490E-06	2.719E-06	3.104E-06	7.714E-07	12.42564991
Total System	5.681E-07	3.044E-07	4.363E-07	2.637E-07	30.2267491
Note	For Torsion Rod, max. flexibility corresponds to post-treatment. For Total System, max. flexibility corresponds to pre-treatment.				

## **Repeatability Test**

The results presented Figure 10-Figure 13 and Table 2 and Table 3 suggest that data obtained from tap tests when all test conditions are held constant from one trial to the next is very consistent and repeatable. Even including outlier measurements as a worst-case scenario, it is observed that the range of identified frequencies for a given sample of measurements is on the order of 1 Hz, which is insignificant except for measurements in the very low frequency range. This view is supported by the percent relative difference reported in the above tables.

This result is not surprising as the FRF produced by each tap test is the result of averaging multiple measurements of the impulse response of the system under investigation. Furthermore, the tap test software provides feedback to the user if a given hammer impulse is faulty, and the user has the option of reviewing each measurement of the impulse response before rejecting or including it in the overall results of the tap test.

In general, sources of error in tap test results include: misalignment (not to be confused with offset) between the impact force and axis of measurement of the accelerometer; incorrect software settings (for example inputting incorrect transducer sensitivities or cutting parameters); undue influence of the dynamics of secondary support structures due to poor fixturing or test setup; noise due to poor electrical grounding or interference; incorrect or faulty mounting of the accelerometer (for example, using an improper amount of adhesive); poor selection of hammer size, hammer tip material, and/or mass extender resulting in insufficient excitation energy; and poor coherence in the FRF resulting from any of the above.

Acceptable coherence is generally held to be in the high 90% range. The coherence for the FRFs obtained during the TorSR treatment experiment and the repeatability tests met this criterion, except for high frequencies for which there was not enough excitation energy and for isolated points in the FRF where the magnitude response is near zero and noise and numerical errors in calculating the FRF dominate. The identified modes considered in this report had excellent coherence.

## **Torsional Stress Relief**

Considering the results of the TorSR treatment experiment in Figure 14-Figure 17 and Table 4 and Table 5, it is first observed that the natural frequency of the torsion rod before and after treatment is consistent, while the same is not true of the total system. This suggests that the treatment influenced the state of the total system but was ineffective in treating residual stresses in the torsion rod. Here it is important to note that the mean values, and therefore also the maximum percent differences, are not suitable metrics for evaluating the results as, unlike before, the sample size for each result is only two.

Those metrics are included only for the sake of completeness. Instead, it is more useful to compare the difference between the natural frequency before and after treatment (Max – Min, or range) to the expected difference between consistent results. Normalizing each range by its corresponding mean value (which, even if not equivalent to the true expected value, is still representative of its order of magnitude) and then scaling the resulting values by the normalized range for the repeatability tests yields the results in Table 6 and Table 7. Sample calculations for the Torsion Rod natural frequency follow:

$$Normalized\ Range = \frac{Max - Min}{Mean} = \frac{1.46\ Hz}{628.42\ Hz} = 0.002323 \tag{2}$$

$$Scaled\ Normalized\ Range = \frac{Normalized\ Range}{Normalized\ Range, Tests\ 1 - 5} = \frac{0.002323}{0.001737} = 1.3374 \tag{3}$$

Table 6: Normalized range of natural frequencies

	Range (Hz)	Normalized Range (-)	Scaled Normalized Range (-)
Repeatability Test (Tests 1 - 5)	1.1	0.001737	1
TorSR Treatment, Torsion Rod	1.46	0.002323	1.34
TorSR Treatment, Total System	17.58	0.010431	6.00

Table 7: Normalized range of flexibilities

	Range (m/N)	Normalized Range (-)	Scaled Normalized Range (-)
Repeatability Test (Tests 1 - 5)	2.073E-07	0.10	1
TorSR Treatment, Torsion Rod	7.714E-07	0.25	2.54
TorSR Treatment, Total System	2.637E-07	0.60	6.18

The results in the above tables confirm that the natural frequency of the torsion rod before and after the stress relief treatment is fairly consistent while that of the total system is not. This implies that the treatment was not effective in relieving residual stress in the torsion rod. During the experiment it was noted that the test specimen was indeed excited, but that the mode of vibration was consistently not torsional. This may explain why the treatment was not effective.

Conversely, the above results also imply that the treatment was “effective” in relieving residual stress in the total system. If the state of the total system was altered but that of the torsion rod was not, then the observed shift in natural frequency must be due to changes in parts of the system other than the torsion rod. Considering the placement of the accelerometer and hammer impacts during the tap tests, one explanation is that the impulse imparted by the hammer was insufficient to excite the entire system, or experimental set-up, and that the observed FRFs are dominated by the dynamics of the Torsion Bar (the

moment arm connecting the test specimen to the vibrator, see Figure 1). This argument is supported by the fact that the Torsion bar is not a rolled part and is characteristic of specimens that have been successfully treated by conventional VSR in the past.

Sources of error include those identified for the Tap Test Repeatability experiment, and factors related to the fixture design that have already been identified in the experiment debrief. Furthermore, although a reasonable effort was made to guard against error and a review of the analysis was undertaken, there is the possibility that calculation errors were introduced into the Excel spreadsheets due to issues where Excel would crash. Similarly, it should be noted that the natural frequencies identified in the interim results (presented again in the Background section of this report) are not formally local maxima, but rather attempts at locating the maxima using the mouse pointer. The natural frequencies that were identified in subsequent sections of this report are in fact at local maxima, however. Finally, the observed changes in flexibility may offer additional insight into the TorSR treatment and reveal additional sources of error or challenges to be addressed. For the sake of brevity, the discussion on the variance in the magnitude response of the FRFs is left for a later work.

### **10.9 Conclusion on tap testing**

The results of an experiment designed to evaluate the repeatability of tap tests were evaluated, and these results were used to interpret FRFs measured during the TorSR experiment. The results of the former experiment show that results obtained from tap tests are in fact repeatable for consistent testing conditions. The consistency of the successive tap tests was then used as a base line to evaluate data obtained during the TorSR experiment. Analysis of the data shows that there was no significant change in the natural frequency of the test specimen but that there was a measurable change in the natural frequency of the experimental setup. While discussing routine sources of error in the data, an explanation for the results was offered whereby the observed difference in the experimental setup is attributable to changes in the natural frequency of the torsion bar, which was directly exposed to excitations from the vibrator. Furthermore, it was observed during the TorSR experiment that the test specimen was excited by the vibrator, but not necessarily in a torsional mode. It is therefore likely that, due to previously stated limitations of conventional VSR treatments, the torsion rod was resistant to stress relief treatment, whereas the torsion bar is more amenable to conventional VSR.

Considering the above observations, for future TorSR treatment experiments it is recommended that

1. Adjustments be made to the fixture used in the experiment and additional analysis be carried out to ensure that the torsion rod does in fact experience torsional vibration.
2. If the dynamics of the experimental setup are to be determined, multiple tap tests with various locations and configurations of impact location and accelerometer placement be conducted so that the system can be characterized by a multi-input, multi-output (MIMO) model. In this way, the dynamics of a single component of the experimental setup will not dominate the frequency response function of the entire system.
3. When conducting tap tests of the test specimen it is removed from the experimental set up.

Five tap tests each consisting of obtaining five impulse response measurements were conducted under identical test conditions. The subsequent analysis of the data demonstrated that the results obtained by tap tests are indeed repeatable and consistent. For an identified first mode of vibration on the order of 630 Hz, the spread of sample points of natural frequencies was considered. It was found that the greatest difference between any two sample points was on the order of 1 Hz and that the maximum relative difference from the expected natural frequency was 0.12%.

These results were used as a baseline to formally evaluate the results of the TorSR experiment. It was determined that the TorSR treatment caused a significant shift in the natural frequency of the experimental set-up but not in the torsion rod (test specimen) itself. This was attributed to the fact that the vibration experienced by the test specimen was not strictly torsional and that it has been previously documented that rolled and cylindrical parts are resistant to conventional VSR treatment, hence the need for this project. Furthermore, observed changes in the FRF of the entire system can be attributed to changes in the torsion bar (moment arm) due to its close proximity to the vibrator causing the excitation, the fact that the torsion bar is similar to a part that could be treated by conventional VSR, and also the fact that the tap test of the experimental setup likely did not impart enough energy to excite the entire system and the observed FRF was dominated by the dynamics of the torsion bar.

Considering the above findings, a number of recommendations are made in the conclusion of this report, of which one is to perform additional analysis to ensure that the mode of vibration experienced by the test specimen is in fact torsional.

1. Adjustments be made to the fixture used in the experiment and additional analysis be carried out to ensure that the torsion rod does in fact experience torsional vibration.
2. If the dynamics of the experimental setup are to be determined, multiple tap tests with various locations and configurations of impact location and accelerometer placement be conducted so that the system can be characterized by a multi-input, multi-output (MIMO) model. In this way, the dynamics of a single component of the experimental setup will not dominate the frequency response function of the entire system.
3. When conducting tap tests of the test specimen when it is removed from the experimental set up, that the test be done with the specimen suspended rather than resting on the ground or on a platform.

It was decided to remove the test specimen from the test set-up when doing the tap testing and thereby removing several potential uncertainties.

## **11 Results of torsional and flexural tests**

Result of performed tests is presented in this chapter including results of tests of reference bars which have received no treatment or treat with flexural vibration. The reason for testing the latter two type of bars is to validate an effect of a treatment and to quantify if the TorSR treatment is more efficient than the more standard flexural vibration.

### **11.1 Results of testing Ø50 mm bars**

The Ø50 mm bars have been subjected to following steps to determine if stresses can be relieved by torsion:

- 1. Taptesting
- 2. Torsion treatment
- 3. Taptesting
- 4. Thermal stressing
- 5. Taptesting
- 6. Torsion treatment
- 7. Taptesting

Results presented in this section represents the taptests made through the course of the outlined steps.

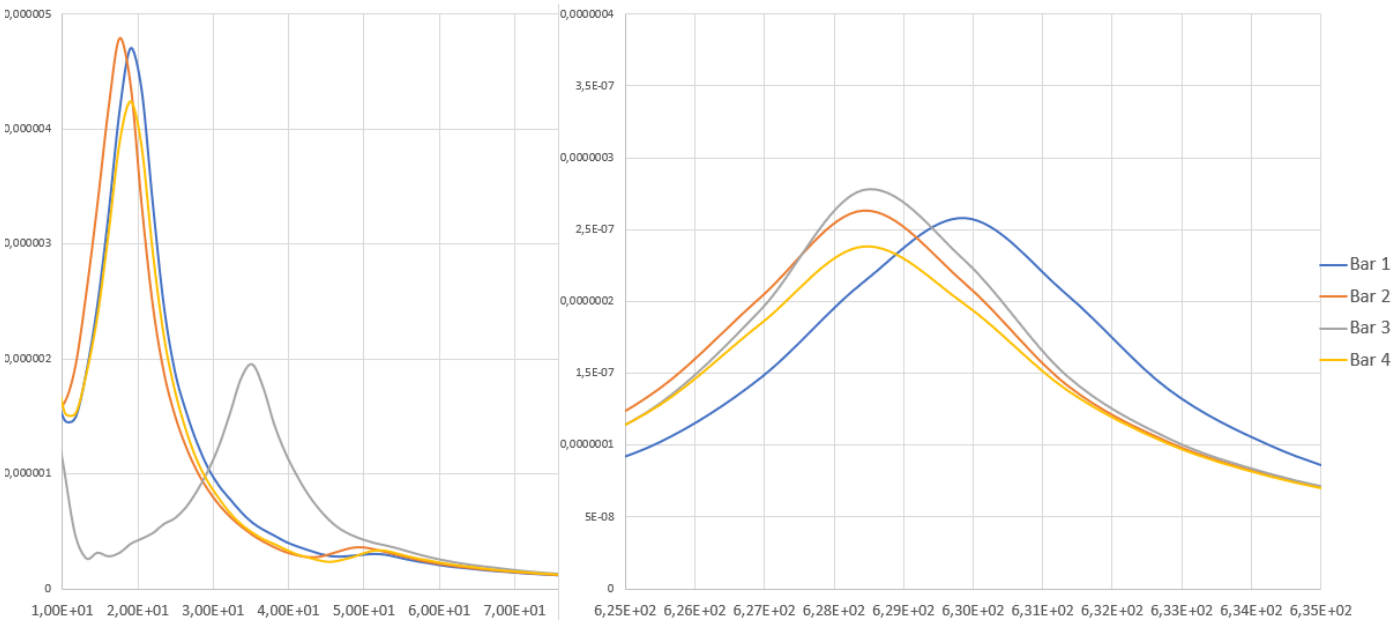


Figure 18: Characterization of four bars.

For understanding the nature of the bar materials in terms taptesting natural frequencies, four bars were tested. Mode 0, left side graph shows some variation but is assumed to be an inconsistency in the measurement. On the right-side graph, the max values of the four bars for mode 1, which is the primary interest for torsion, indicating the resonance frequencies is quite closely positioned. The bars seem quite uniform in the resonance frequencies.

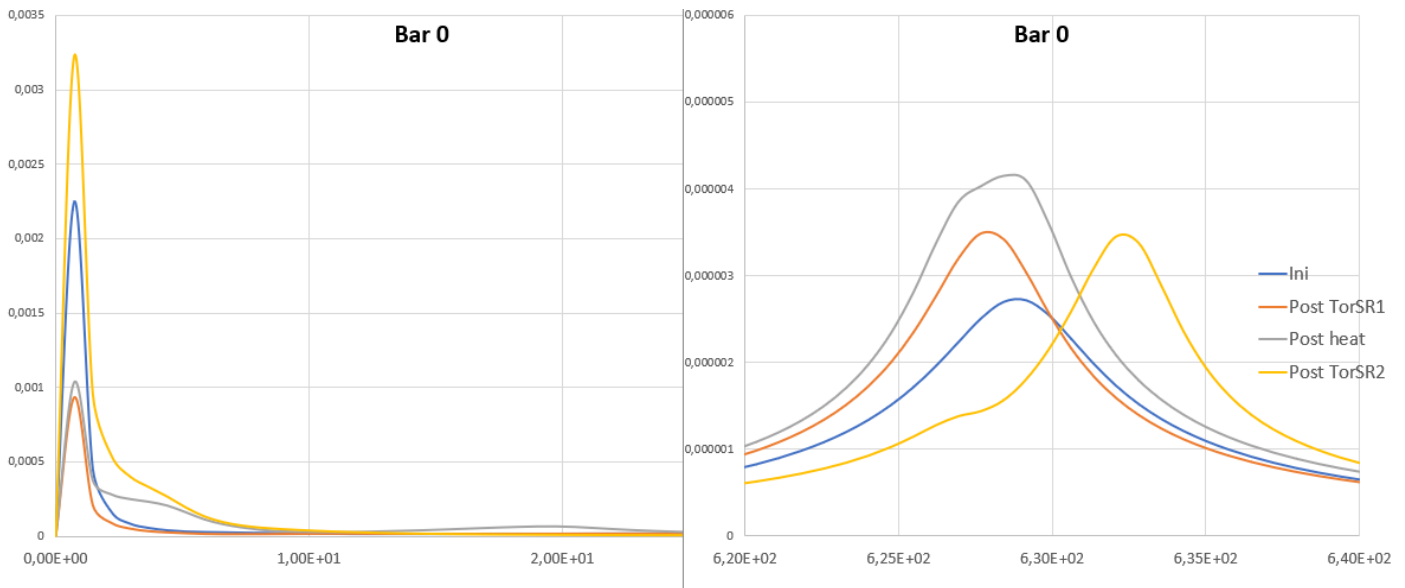


Figure 19: Results of testing bar 0. Magnitude as a function of frequency (x axis).

The result of testing the bar numbered 0 is presented in figure 7. In theory, the blue and grey curves should have maximum at highest frequencies and yellow and orange curves have maximum at lowest frequencies. The result though, is not showing a clear agreement with the expectations from theory. The orange curve, indicating the state of stresses after first torsional treatment has a slightly lower max frequency than the curves for initial and post thermal stressing. The yellow curve which ideally should be coinciding with the orange curve has max at even bigger frequencies than ini(tial) and post heat curves. The reason for the disagreement may be due to various reasons:

- The stresses in the bars, both as delivered and the stress thermally induced after first round torsional treatment were not big enough to generate a significant change in residual stress in the bar compared to the accuracy of tap testing,
- The torsional treatment was not able to reduce stresses so significantly that a clear change is visible on the graphs. This is also discussed in appendix 2 on repeatability of taptesting.

The conclusion is that it is probably due to a combination of both aforementioned reasons that a clear indication the effect of the torsional treatment. For this reason, it is decided not to test the four other bars since they were very similar to the bar 0 and then similar results would be expected.

## 11.2 Results of testing Ø25 mm long bars

In the experiment design section, it is outlined that 2 Ø25 mm bars of app. 3000 mm length are tested. The rationale of testing long slim bars is to investigate the effect of various aspect ratios. The test sequence of the two bars is:

1. Taptesting
2. Torsion/flexural treatment
3. Taptesting

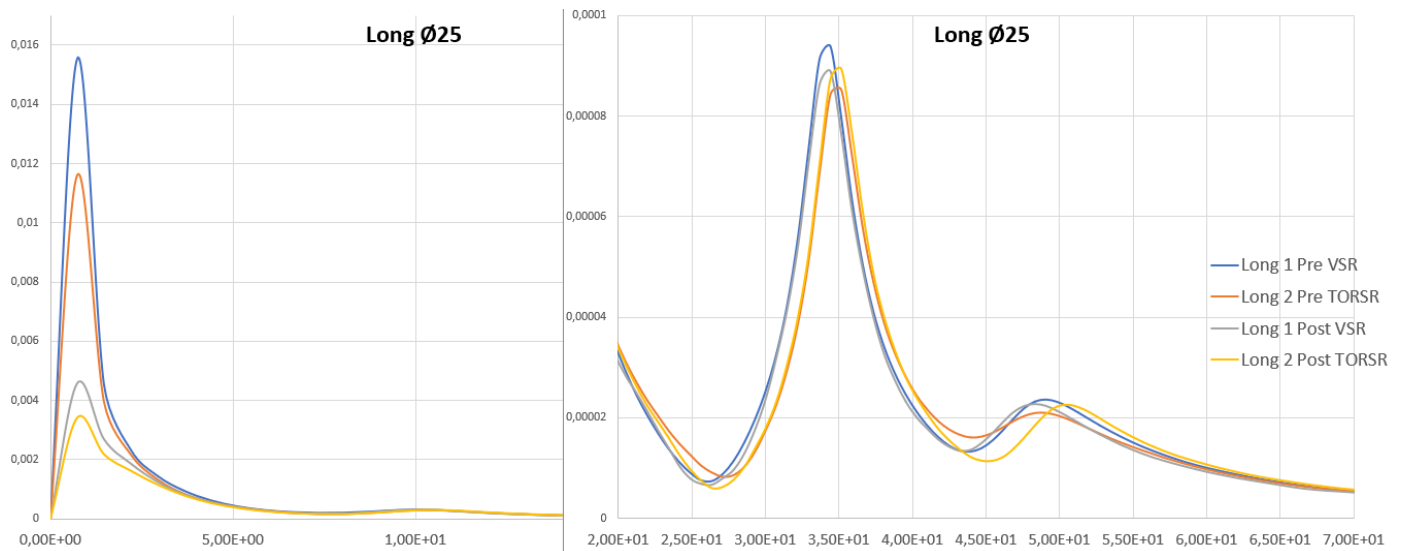


Figure 20: Result of testing Ø25 mm long bars before and after torsion treatment.

Figure 8 shows both taptest results of effect of VSR (flexural) treat and torsional treatment. Blue and green curves are pre and post VSR treatment and yellow and orange curves are pre and post torsional treatment. In both cases the change from pre to post treatment of the position of the peak magnitude is so small that it is not visually detectable. In theory, the bars as delivered from the supplier in cold drawn state should have stresses that could be relieved. Despite that stresses should be prevalent in the bars neither torsional nor flexural vibration were able to show any change in the mode 1 resonances of the bars. Now, since it is not known how large stresses to expect in the supplied bars, it is difficult to state with certainty that neither of the treatments have no effect. In the test of the short Ø 25 mm bars, efforts are made to induce stresses.

### 11.3 Results of testing Ø25 mm short bars

The Ø25 mm bars were tested as the sequence listed below:

1. Induce stress
2. Taptest
3. Torsional vibrations
4. Taptest

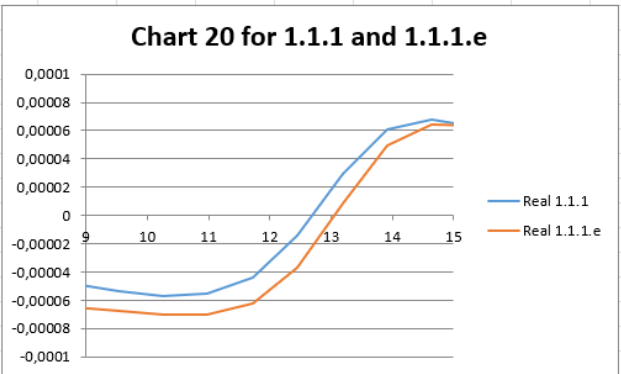
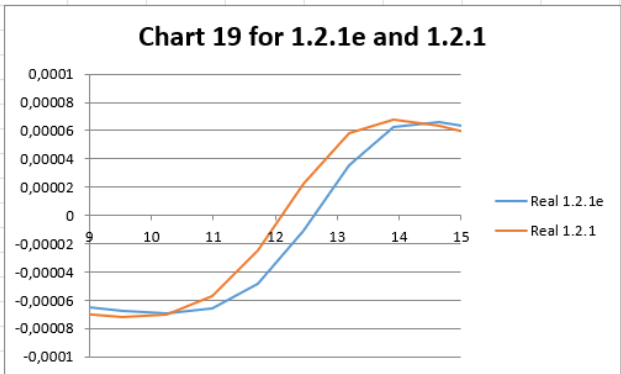
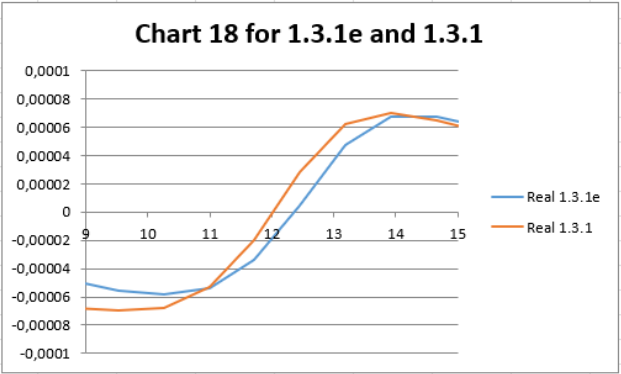
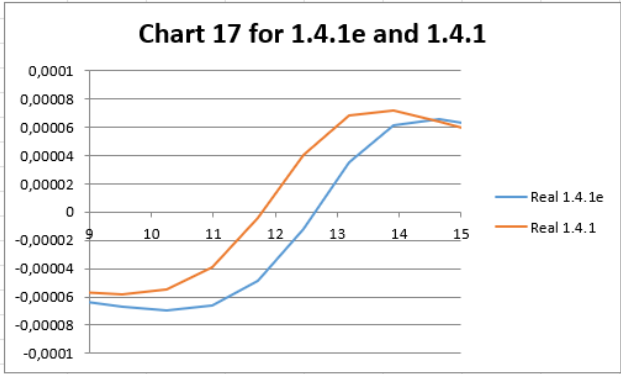
#### Taptest before and after treatment

The taptest before torsional treatment was done with the ends on foam cushions, to stabilize them. They tended to roll when tap testing them on a harder surface. The tests were conducted four times around the center circle. The naming of the test 1.2.1e means: 1. bar, 2. Quadrant impact spot, 1 test (two tests were done on the first rod to determine operational difference), e means test after treatment or after control (no treatment). 1 and 3 are treated, 2 and 4 are controls. An example of bar 3 before and after torsional treatment is presented in figures 9-12. Each subgraph below represents a taptest before and after torsional treatment. Please see appendix 3 for all taptest on the four bars. As a reference bar 2 and 4 is not subjected to vibration.

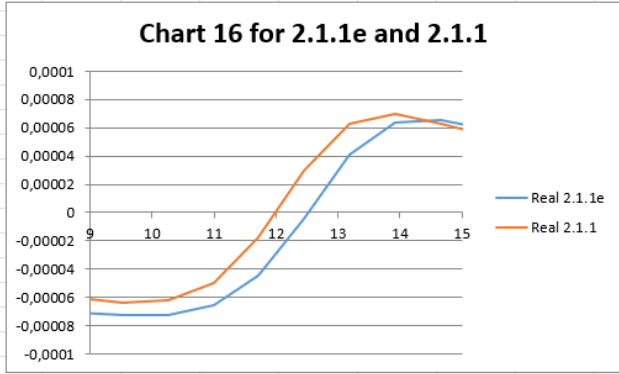
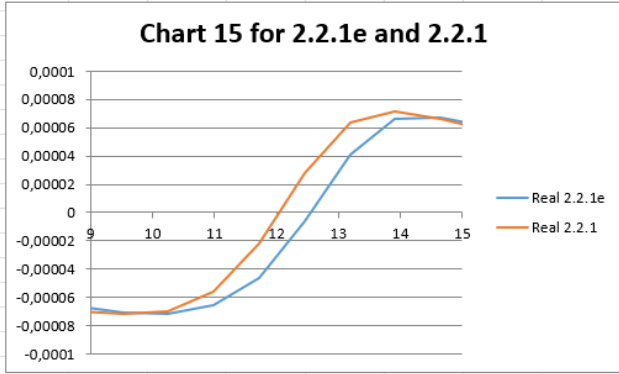
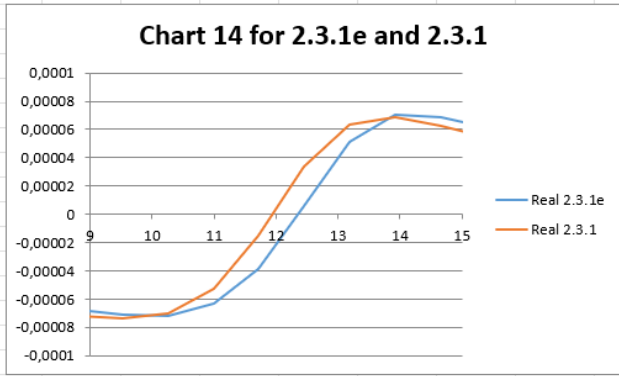
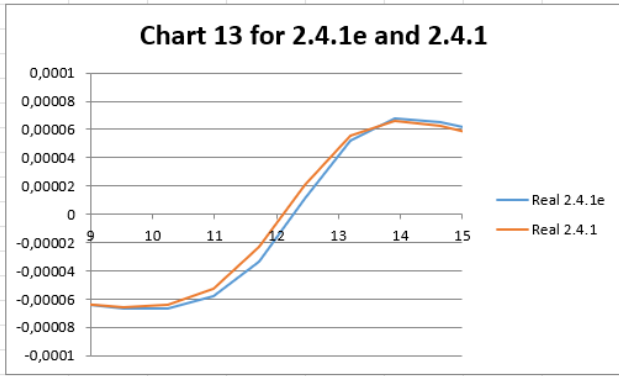
To be able to judge the results with higher certainty four taptests were made before and after treatment on each bar. In the following section the graphs of the taptesting of each bar is presented. The focus on

analysis the resulting graphs is the gap in frequency (horizontal axis) between the red and the blue curve. The bigger the gap, the higher the effect of treatment and the smaller the gap between the curves of the controls the more certain the effect is of the treatment.

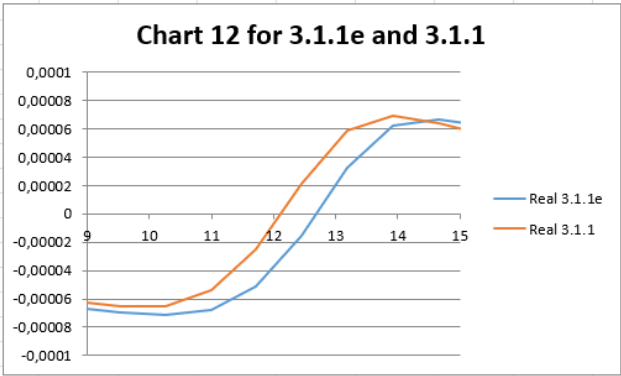
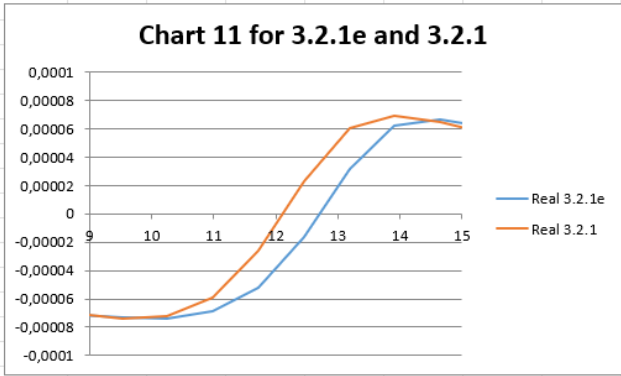
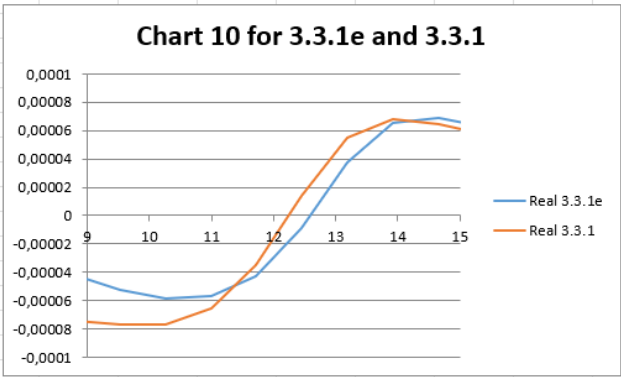
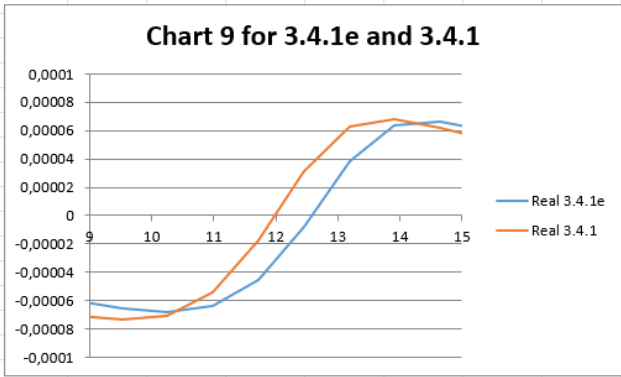
### 11.4 Test of 1. rod before and after treatment



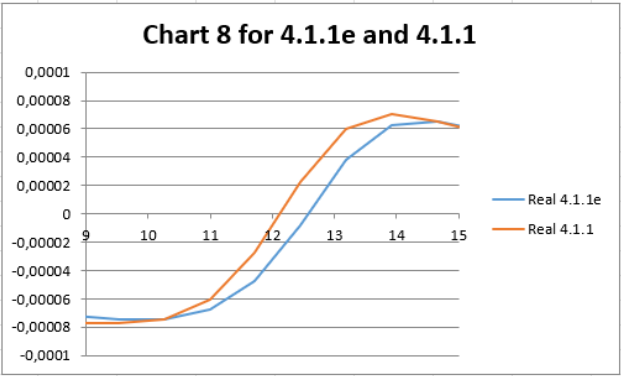
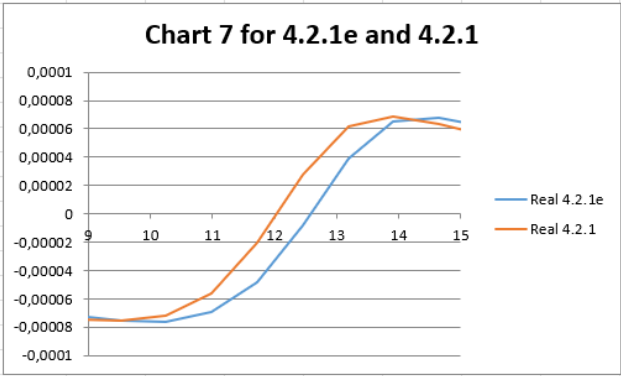
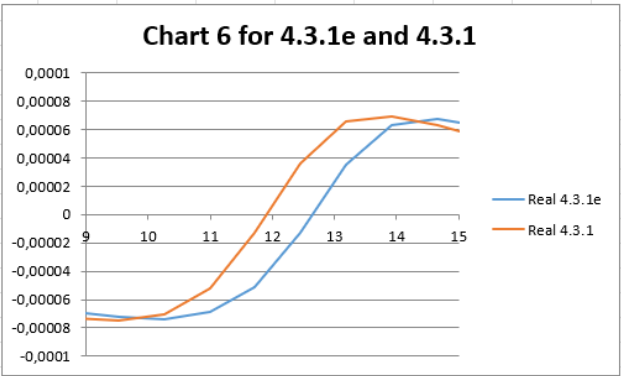
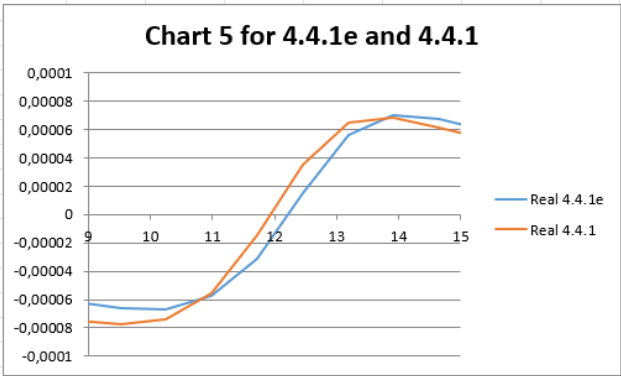
### 11.5 Test of 2. Rod (control)



## 11.6 Test of 3. Rod after treatment



## 11.7 Test of 4. Rod (control)



## 11.8 Analysis of test results

Overall, the test results are consistent but in disagreement with theory anticipating reduction in residual stress, i.e.:

- All the rods have larger changes than the immediate testing variance, even the controls.
- Almost all the rods are measured to have higher resonance frequencies which is not consistent with materials theory – could indicate that the treatment rather induced stresses in the material than reducing them.
- The control bars seem to exhibit the same pattern as the treated bars and thus there is no evidence of differences between the test and the controls which indicates that either the stressing of the bars was unsuccessful or the that the torsion treatment was unsuccessful.
- The taptesting measurement on 4 positions on the bars also showed quite big variations which questions the capability of this method on stress quantification.

## 12 Discussion

Three series of test were made in order to show the capability of torsion treatment of residual stresses. These test series were designed to investigate effect the aspect ratio and partly also to show the effectiveness of torsional versus flexural (VSR) residual stress treatment. The cold drawn bars should have stress already when delivered. Though, since the bars have been on stock for some time before delivered to DAMRC it is not known to which degree they still had significant residual stresses when tested since DAMRC does not have equipment to measure stresses. To ensure that stresses were present at the testing, efforts were made to induce stresses in the bars. These efforts were of both thermal and mechanical type and are both well known to cause stresses in materials in many cases.

It was not possible to demonstrate a reduction in residual stress neither through torsional nor flexural treatment of the bars when compared to no treatment at all. This, despite various efforts on ensuring the success of treatment already in the planning phase with e.g. characterisation of vibrator through tests and finite element (FEM) analysis of the necessary load to achieve large enough loads on the bars to obtain stress relaxation.

There are mainly three questions to be contemplated after the tests, were there at all significant residual stresses to reduce present in the bars, is the torsional and flexural vibration capable of reducing stresses in these bars and is the taptesting method a reliable way of indicating changes in residual stress? The answer on these questions were not demonstrated reliably through the testing. In some of the tests it seemed that there was a positive effect of the torsional vibration but too small for the taptesting to demonstrate clearly. Validating the taptest equipments capability of reducing residual stresses or making use of other methods for stress measurement is crucial for later tests of residual stress reduction. Further, more elaboration on results achieved externally on which materials that can be stress relieved can be a way to ensure that a clear result can be achieved.

## 13 Conclusion

The conclusion on the tests carried out in this project is that in some of the tests a positive effect of torsional stress relief may have been achieved but that it was too small for the tap testing equipment to indicate in a reliable way. In some of the tests no effect was demonstrated and the effectiveness of torsional versus flexural vibration was not demonstrated neither.

## 14 Dissemination

Announcement on DAMRC web of the Project launch

MADE: 2<sup>nd</sup> meeting in Production network. @ Baettr. Presentation including TorSR. April 4<sup>th</sup>, 2023.

VTM 2023: Industrial fair in Odense. Presentation including TorSR at fair on April 27<sup>th</sup>. TorSR also presented at the DAMRC stand.

MADE: Virtual Deep dive on stresses in metals. On-line. Presentation including TorSR June June 23<sup>rd</sup>, 2023.

Meeting with Weldcast consortium. Intro to stress relief by vibration. September 9<sup>th</sup>, 2023

Visit from DI KSL (Kjøbenhavns smedelaug). Demo of vibration technologies for stress relief, October 11<sup>th</sup>, 2023.

Teknologi og tendenser. Tech fair at DAMRC. Demo of vibration technologies. November 28<sup>th</sup>, 2023.

## 15 References

- A S M Y Munsif, A. J. (01. 01 2001). Vibratory stress relief—an investigation of the torsional stress effect in welded shafts. *The Journal of Strain Analysis for Engineering Design*, 5, s. 453-464. doi:10.1243/0309324011514610
- Cai, G. &. (2. 10 2017). Operating principle of vibratory stress relief device using coupled lateral-torsional resonance. *Journal of Vibroengineering*, 19(6), s. 14. doi:10.21595/jve.2017.18221
- Walker, C. W. (01. 02 1995). Vibratory Stress Relief—An Investigation of the Underlying Processes. , 209, 51 - 58. *Proceedings of the Institution of Mechanical Engineers, Part E: Journal of Process Mechanical Engineering*, 1, s. 51-58. Hentet fra [https://doi.org/10.1243/PIME\\_PROC\\_1995\\_209\\_228\\_02](https://doi.org/10.1243/PIME_PROC_1995_209_228_02)

## 16 Appendix: Order confirmation Ø25 mm bars



DK-3300 Frederiksværk - Telefon +45 47767600

**TIBNOR A/S**  
 Klokkestøbervej 18, 2.  
 DK-5230 - Odense  
 DANMARK

Lieferbedingung / Specification:  
**EN 10277 S355J2C+C Sulph**

### BESCHEINIGUNG / CERTIFICATE

Stabstahl/Bars

Seite / Page: 1/1 Nr./No.: **141986**

Type: **EN 10204 / 3.1**

Ihrer Auftrag/Your order: **46377610-0450**

Uner Auftrag/Our order: **76866**

Datum/Date: **13-04-2023**

Lieferstelle/Delivery address:

**Tibnor A/S**  
 Prinsessens Kvarter 5  
 DK-7000 - Fredericia  
 DANMARK

Toleranz Tolerance: **EN 10278 TOLL. H9**

Pos.	Product Type	Abmessungen/Dimensions										Stk/Pcs	Gewicht/Weight	Schmelze/Heat	Lieferzustand/Condition of delivery		
1	Rund	3000										1	1003	43372	Wabzustand / As rolled		
2	Rund	3000										4	3990	44518	Kenzeichnung/Marking		
3															Sachverständigen/Quality inspector:		
4															Schmelzverfahren: 10.000-29.000 Konverterverfahren/Oxygen converter		
5															30.000-99.999 Elektro-Ofen/El-arc-furnace		
6															Im Phosphoraffiniert/affine refined		
7																	
8																	
9																	
10																	
Total weight												<b>4993</b>					
	C	Mn	Si	P	S	Cr	Cu	Ni	Mo	Sn	Al	Nb	Ti	V	B	N	CEq = Carbon-Equivalent (IIRW - formula)
1	19	108	21	17	31	11	17	7	2		31	0	1	22		41	42
2	17	109	24	9	37	6	15	8	2		26	0	2	32		87	39
3																	
4																	
5																	
6																	
7																	
8																	
9																	
10																	
	% x 100		% x 10000		% x 100			% x 10000			% x 10.000		% x 100				
	Zugversuch/Tensile test			Kerbschlagbiegeversuch/Impact test/ISO - V					Hardness	DDS requires, that all billet suppliers make statement in writing to the effect, that the billets delivered have not been exposed to and/ or contaminated with radiation.							
	ReH	Rm	A5	1	2	3	Misr/Average	Temp	Bei Material mit einer Dicke unter 10 mm, werden die Kerbschlagproben zu einer Breite von entweder 7.5 mm oder 5.0 mm bearbeitet.								
1	630	660	14						For material with thickness less than 10 mm, the impact testpieces are machined to a width of either 7.5 mm or 5.0 mm.								
2	685	730	10														
3																	
4																	
5																	
6																	
7																	
8																	
9																	
10																	
	MPa		%	Joule			°C	HB									

Wir bestätigen, dass die Lieferung den Anforderungen der obengenannten Lieferbedingungen und des Auftrages entspricht.  
 We hereby certify, that the material has been produced and tested in compliance with the mentioned specification and with the requirement of the order.

Dufenco Danish Steel A/S

Mauro Buccioli  
 Quality Department

List of Figures

Figure 1: Test set-up for torsional vibration treatment of bars. ....9

Figure 2: Geometry of the system. ....10

Figure 2 - Modes of Vibration. ....11

Figure 3: Modes of vibration.....11

Figure 4: Air valves device.....12

Figure 5: Pneumatic motor - Vibration analysis. ....12

Figure 7: Polynomic regression model.....13

Figure 10, Ø25 mm bar test set-up. Silver VSR vibrator mounted on torsional arm. Bar is fixed in one end and supported with a bearing in the other end. This set-up is used both for app. 3000 mm bar and app. 1500 mm bar. The vibrator is balanced vertically to eliminate static load and hereby also overload of the bar. ....17

Figure 11: flexural vibration set-up. The bar is supported 2/3 from the end. ....18

Figure 12: thermal stressing of bar with propane gas flame.....19

Figure 13: demonstration of the small deflection after bending. ....19

Figure 1: 3D rendering of the experimental setup. Note that in the experiment the end of the rod opposite the torsion bar has a fixed boundary condition. ....20

Figure 2: Placement of the test specimen during tap tests when removed from the experimental set-up..20

Figure 3: Comparison of the first identified mode of the Torsion bar before and after treatment. There are minor cosmetic and formatting changes to this, and the following graphs compared to the interim results presented previously. ....21

Figure 4: Percent change in the magnitude response of the FRFs in the previous graph.....22

Figure 5: Comparison of the first identified mode of the experimental set up before and after treatment. 22

Figure 6: Percent change in the magnitude response of the FRFs in the previous graph.....23

Figure 7: Accelerometer and impact location on the torsion rod. Marks made on the rod during its manufacture are used to pinpoint the loation of the hammer taps. ....24

Figure 8: The resonance peak of the first mode obtained from each tap test. ....25

Figure 9: Detailed view of the FRFs from the previous figure. ....26

Figure 10: "Box and Whisker" plot showing the spread of the first identified natural frequency. ....26

Figure 11: "Box and Whisker" plot showing the spread of the magnitude response at each identified natural frequency. ....27

Figure 12: The spread of the identified natural frequencies is displayed with test 1 omitted. ....27

Figure 13: The spread of response magnitude at the identified natural frequencies with test 1 omitted. ...28

Figure 14: Box and Whisker plot of Torsion Rod natural frequencies.....29

Figure 15: Box and Whisker plot of Torsion Rod Flexibilities .....29

Figure 16: Box and Whisker plot of Total System natural frequencies .....30

Figure 17: Box and Whisker plot of Total System flexibilities .....30

Figure 14: Characterization of four bars. ....35

Figure 15: Results of testing bar 0. Magnitude as a function of frequency (x axis). ....36

Figure 16: Result of testing Ø25 mm long bars before and after torsion treatment. ....37

Figure 17: Graphs on bar 3 after torsional treatment. Frequency in Hz on X-axis.....**Fejl! Bogmærke er ikke defineret.**

## List of Tables

Table 1: Natural frequencies.....	11
Table 2: Summary of data (identified natural frequencies) in Figures 10 and 12 .....	28
Table 3: Summary of data (flexibility at identified natural frequencies) Figures 11 and 13 .....	28
Table 4: Key data from Figures 14 and 16 .....	30
Table 5: Key data from Figures 15 and 17 .....	30
Table 6: Normalized range of natural frequencies .....	32
Table 7: Normalized range of flexibilities .....	32

## 17 Bibliografi

- A S M Y Munsj, A. J. (01. 01 2001). Vibratory stress relief—an investigation of the torsional stress effect in welded shafts. *The Journal of Strain Analysis for Engineering Design*, 5, s. 453-464.  
doi:10.1243/0309324011514610
- Cai, G. &. (2. 10 2017). Operating principle of vibratory stress relief device using coupled lateral-torsional resonance. *Journal of Vibroengineering*, 19(6), s. 14. doi:10.21595/jve.2017.18221
- Walker, C. W. (01. 02 1995). Vibratory Stress Relief—An Investigation of the Underlying Processes. , 209, 51 - 58. *Proceedings of the Institution of Mechanical Engineers, Part E: Journal of Process Mechanical Engineering*, 1, s. 51-58. Hentet fra [https://doi.org/10.1243/PIME\\_PROC\\_1995\\_209\\_228\\_02](https://doi.org/10.1243/PIME_PROC_1995_209_228_02)